

## Intranasal delivery of sulpiride nanostructured lipid carrier to central nervous system; in vitro characterization and in vivo study

Hesham M. Tawfeek, Aml I. Mekkawy, Ahmed A. H. Abdelatif, Basmah N. Aldosari, Waleed A. Mohammed-Saeid & Marwa G. Elnaggar

**To cite this article:** Hesham M. Tawfeek, Aml I. Mekkawy, Ahmed A. H. Abdelatif, Basmah N. Aldosari, Waleed A. Mohammed-Saeid & Marwa G. Elnaggar (2024) Intranasal delivery of sulpiride nanostructured lipid carrier to central nervous system; in vitro characterization and in vivo study, *Pharmaceutical Development and Technology*, 29:8, 841-854, DOI: [10.1080/10837450.2024.2404034](https://doi.org/10.1080/10837450.2024.2404034)

**To link to this article:** <https://doi.org/10.1080/10837450.2024.2404034>



Published online: 24 Sep 2024.



Submit your article to this journal [↗](#)



Article views: 24



View related articles [↗](#)



View Crossmark data [↗](#)

RESEARCH ARTICLE



## Intranasal delivery of sulpiride nanostructured lipid carrier to central nervous system; in vitro characterization and in vivo study

Hesham M. Tawfeek<sup>a</sup> , Aml I. Mekki<sup>b</sup>, Ahmed A. H. Abdelatif<sup>c</sup>, Basmah N. Aldosari<sup>d</sup>, Waleed A. Mohammed-Saeid<sup>e</sup> and Marwa G. Elnaggar<sup>a,f</sup>

<sup>a</sup>Department of Industrial Pharmacy, Faculty of Pharmacy, Assiut University, Assiut, Egypt; <sup>b</sup>Department of Pharmaceutics and Clinical Pharmacy, Faculty of Pharmacy, Sohag University, Sohag, Egypt; <sup>c</sup>Department of Pharmaceutics, College of Pharmacy, Qassim University, Buraydah, Saudi Arabia; <sup>d</sup>Department of Pharmaceutics, College of Pharmacy, King Saud University, Riyadh, Saudi Arabia; <sup>e</sup>Department of Pharmaceutics and Pharmaceutical Industries, College of Pharmacy, Taibah University, Madinah, Saudi Arabia; <sup>f</sup>Department of Industrial and Molecular Pharmaceutics, Purdue University, West Lafayette, IN, USA

### ABSTRACT

The low and erratic oral absorption of sulpiride (SUL) a dopaminergic receptor antagonist, and its P-glycoprotein efflux in the gastrointestinal tract restricted its oral route for central nervous system disorders. An intranasal formulation was formulated based on nanostructured lipid carrier to tackle these obstacles and deliver SUL directly to the brain. Sulpiride-loaded nanostructured lipid carrier (SUL-NLC) was prepared using Compritol® 888 ATO and different types of liquid lipids and emulsifiers. SUL-NLCs were characterized for their particle size, charge, and encapsulation efficiency. Morphology and compatibility with other NLC excipients were also studied. Moreover, SUL *in vitro* release, nanodispersion stability, *in vivo* performance and SUL pharmacokinetics were investigated. Results delineates that SUL-NLC have a particle size ranging from  $366.2 \pm 62.1$  to  $640.4 \pm 50.2$  nm and encapsulation efficiency of  $75.5 \pm 1.5\%$ . SUL showed a sustained release pattern over 24 h and maintained its physical stability for three months. Intranasal SUL-NLC showed a significantly ( $p < 0.01$ ) higher SUL brain concentration than that found in plasma after oral administration of commercial SUL product with 4.47-fold increase in the relative bioavailability. SUL-NLCs as a nose to brain approach is a promising formulation for enhancing the SUL bioavailability and efficient management of neurological disorders.

### ARTICLE HISTORY

Received 9 May 2024  
Revised 5 August 2024  
Accepted 10 September 2024

### KEYWORDS

Sulpiride; Nanostructured lipid carrier; nose to brain delivery; Nanoparticles; relative bioavailability

## 1. Introduction

Despite the increasing global prevalence of central nervous system (CNS) disorders, drug delivery to the brain remains a tough endeavour (Kim et al. 2019). The challenge is primarily attributed to the defense by physiological and anatomical barriers, particularly the blood brain and the blood cerebrospinal fluid barriers, which influence drug delivery and are considered a crucial hurdle in developing therapies for CNS disorders (Achar et al. 2021; Terstappen et al. 2021; Nance et al. 2022).

Intranasal (IN) drug delivery is a compelling method for achieving elevated drug concentrations in the brain (Formica et al. 2022). Drugs' Nose-to-Brain passage primarily occurs through the systemic, olfactory, and trigeminal nerve pathways (Bourganis et al. 2018; Deshkar et al. 2021). Furthermore, it is a non-invasive route with enhanced patient compliance, rapid onset of action as well as higher blood perfusion and targeted delivery concomitant with avoiding the hepatic circulation degradation (Patel et al. 2011; Kozlovskaya et al. 2014; Bourganis et al. 2018).

Lipid nanocarriers are widely preferred materials for brain targeting regarding their biocompatibility, rapid uptake and lower toxicity (Kozlovskaya et al. 2014; Singh et al. 2016). It has been proven that lipid-based nanoparticles like solid lipid nanoparticles (SLNs) and nanostructured lipid carriers (NLCs) have shown promise nanocarriers for efficient nasal delivery for many drugs (Khan et al. 2016; Singh et al. 2016; Rassa et al. 2017; Jicsinszky et al.

2021). NLCs are used extensively as a promising carrier for nose-to-brain delivery as reported from literatures (Noorulla et al. 2022; Yasir et al. 2022).

NLCs emerged in the late 1990s as a promising evolution beyond SLNs, addressing potential challenges associated with SLNs. NLCs enhance stability, increase drug loading capacity, mitigate the risk of drug expulsion during storage, and provide uniform drug distribution and smaller particle size (Pardeike et al. 2009; Patel et al. 2013). It has been reported that NLCs could improve the low oral bioavailability of carvedilol *via* nasal delivery. Authors reported that the formulated IN formulation had a significantly higher bioavailability compared with oral formulation (Aboud et al. 2016).

Sulpiride (SUL) is a dopaminergic receptor antagonist with wide therapeutic applications in the CNS for instance, schizophrenia and major depressive disorder (Nakazato et al. 1998; Ayub 2016; Kim et al. 2016; Mohyeldin et al. 2021). SUL has a low solubility and permeability exhibiting a class IV-level in the biopharmaceutical systems which contributed to a limited oral bioavailability (approximately 30%) (Parikh et al. 2010; Chitneni et al. 2011). Hence, higher doses of the drug are needed for effective therapy. Within these high doses, patients could suffer from side effects such as sleeping disorders, extrapyramidal and central nervous system side effects (Ibrahim et al. 2014). In addition, it was reported that SUL experiences carrier-mediated efflux facilitated by P-glycoprotein (P-gp) present in different

areas of GIT (Baluom et al. 2001). This phenomenon is implicated in the insufficient bioavailability of SUL following oral administration of approximately 30% (Watanabe et al. 2002; Parikh et al. 2010; Ibrahim et al. 2014). Moreover, it has been reported that SUL has an absorption window in the upper part of GIT which could also worsen the oral absorption (Kohri et al. 1996). Previous studies reported on the enhanced oral bioavailability of SUL after its formulation in floating microsponges (Younis et al. 2020), fast disintegrating tablets (Tawfeek et al. 2020), solid lipid nanoparticles (Ibrahim et al. 2014) and nano-lipospheres (Mohyeldin et al. 2021). Although most of them showed enhanced bioavailability and potential therapeutic efficacy, however, none of those studies have shown the actual potential of brain targeting ability. Moreover, most of these delivery systems based on oral route which still non-convenient for a wide range of patients.

Based on the stated benefits of NLCs as an efficient drug delivery system, together with the high efficacy of IN route for delivery of drugs to the brain could provide a promising way to overcome the problems associated with orally administered SUL and attain the required pharmacological action in CNS.

In this study, SUL-NLCs was developed to enhance the SUL bioavailability and for effective brain targeting through IN pathway. First, SUL-NLCs were prepared using Compritol<sup>®</sup>888 ATO as the solid lipid *via* solvent injection method. Different types of liquid lipids (either oleic acid or labrafac) and different emulsifiers (either Pluronic F-127 (PF-127) or Tween 80 (T80)) with different concentrations were also investigated. SUL-NLCs size, charge and drug encapsulation were evaluated. In addition, SUL-NLC chosen formulation was examined for their morphology, and interaction with lipid carrier *via* FT-IR and DSC. SUL release performance from the chosen SUL-NLC formulation was investigated and SUL-NLC stability was evaluated at different temperatures ( $4.0 \pm 1.0^\circ\text{C}$ ) and ( $25.0 \pm 2.0^\circ\text{C}$ ) for 3 months. SUL pharmacokinetic (PK) parameters were calculated after IN delivery and compared to the orally administrated commercial SUL capsules (Dogmatil<sup>®</sup>) using Sprague-Dawley male rats.

## 2. Materials and methods

### 2.1. Materials

Sulpiride was obtained as a gift from Memphis Pharmaceuticals & Chemical Industries CO (Cairo, Egypt). Compritol<sup>®</sup>888 ATO and labrafac<sup>™</sup> Lipophile WL 1349 were a donation from Gattefossée (Saint-Priest Cedex, France). Poloxamer<sup>®</sup> 407 (Pluronic<sup>®</sup> F-127) was obtained from BASF (Greenville, OH, USA). Oleic acid obtained from Alpha Chemicals Co. (Cairo, Egypt). Tween 80, acetone and ethanol were delivered from El-Nasr Pharmaceutical Chemicals Co. (Cairo, Egypt). Any other chemicals and reagents were of high analytical grade and used as received.

### 2.2. Preparation of sulpiride loaded nanostructured lipid carrier (SUL-NLC)

Table 1 shows the composition of the different prepared SUL-NLCs formulations. Basically, SUL-NLCs were prepared utilizing the solvent injection technique, as mentioned previously by Chen et al. (2012), with some modifications. First, the lipid phase was initially prepared by dissolving 50 mg of SUL, along with 120 mg of solid lipid namely; Compritol<sup>®</sup>888 ATO, and 30 mg of liquid lipid (either oleic acid or labrafac) in approximately two mL of organic solvent mixture formed of acetone/ethanol in a ratio of (3:1 v/v) at a temperature of  $60^\circ\text{C}$ . This is followed by direct injection of lipid phase into 30 ml of preheated aqueous solution of either PF-

**Table 1.** Composition of the prepared SUL-NLC formulations.

No.	Formulation code	Liquid lipid type	Surfactant type	Surfactant %
1	S1	Oleic acid	PF-127	1
2	S2	Oleic acid	PF-127	2
3	S3	Labrafac	PF-127	1
4	S4	Labrafac	PF-127	2
5	S5	Oleic acid	T80	1
6	S6	Oleic acid	T80	2
7	S7	Labrafac	T80	1
8	S8	Labrafac	T80	2

Abbreviations: SUL-NLC: Sulpiride-loaded Nanostructured lipid carrier; PF-127: Pluronic<sup>®</sup> F-127; T80: Tween 80.

127 or T80 (at concentrations of 1% or 2%) as a stabilizer. The resulting mixture was stirred for 3 h at room temperature at a speed of 1000 rpm, using a magnetic stirrer to evaporate the organic solvent. Subsequently, the NLC dispersion was further sonicated for 20 min. The obtained SUL-NLC nanosuspension was stored in fridge for further analysis. Blank NLCs were similarly prepared for testing and comparison.

### 2.3. In vitro characterization of SUL-NLCs

#### 2.3.1. Particle size, polydispersity index and zeta-potential measurements

The average hydrodynamic diameters, size distribution (polydispersity indices, PDIs), and zeta-potential of the prepared SUL-NLCs nanosuspension were performed. Simply, one mg of SUL-NLC dispersed in one ml of double distilled water was prepared then, measured using Zetasizer Nano at room temperature (ZS Nano series, Malvern Instruments, Malvern, UK) (Abdellatif et al. 2021; Aldosari et al. 2023). Polydispersity index indicates the nature of particles distribution either monodisperse and polydisperse system (Jain et al. 2014). The zeta potential was determined using the same instrument with 50  $\mu\text{L}$  of the nanosuspension added to 2 ml of distilled water. The measurement was performed using a gold-plated zeta dip probe at  $25^\circ\text{C}$  (Abdulla et al. 2021). Measurements were performed in triplicates and the average was considered for data analysis.

#### 2.3.2. Encapsulation efficiency

The indirect method (Mekkawy et al. 2022) was employed to calculate SUL encapsulation efficiency of the prepared SUL-NLCs. Briefly, the freshly prepared SUL-NLCs were subjected to centrifugation using centrifugal filters of type Amicon<sup>®</sup> tube Ultra-15 (Mw cut-off = 100 kDa) (Merk Millipore, Darmstadt, Germany), the speed was adjusted to 6000 rpm for 45 min. Subsequently, collected supernatant was analyzed using a UV-VIS spectrophotometer at  $\lambda_{\text{max}}$  of 293 nm (Shimadzu, model UV-1601 PC, Kyoto, Japan). The concentration of SUL was calculated using a previously determined calibration curve. Finally, SUL encapsulated within the NLC was calculated according to this equation:

$$\text{Encapsulation Efficiency (\%)} = \frac{\text{Total Drug Content} - \text{Drug Content in Supernatant}}{\text{Total Drug Content}} \times 100 \quad (1)$$

#### 2.3.3. Morphology

Selected SUL-NLC sample was visualized using the transmission electron microscope (TEM, JEM-1230, Joel Japan). In brief, SUL-NLC nanosuspension was applied to a Formvar-coated grid (300 mesh), stained using 2% uranyl acetate aqueous solution as a negative stain, any remaining solution was removed by absorbing

the liquid with the tip of a piece of filter paper and left overnight to be dried (Abdellatif, Ibrahim, et al. 2020; Abdellatif, Tolba, et al. 2022). Then, the sample was viewed under the microscope at 10–100 k magnification power using an accelerating voltage of 100 kV.

### 2.3.4. Compatibility study

Compatibility study between pure SUL powder, compritol<sup>®</sup>888 ATO, physical mixture of the drug and compritol<sup>®</sup>888 ATO, selected SUL-NLC and blank NLC were obtained using DSC (DSC-50 Shimadzu, Seisakusho Ltd., Kyoto, Japan) and FT-IR spectrometer (Nicolet 6700, ThermoFisher Scientific, Waltham, MA, USA) (Abdellatif, Aldosari, et al. 2022; Abdellatif, Alhathloul, et al. 2022). Briefly, Samples were added into aluminium pans and heated at a scanning rate of 10 °C/min, 30–250 °C in the presence of nitrogen, flow rate set to 40 ml/min. DSC-T50 software 1.01 (Shimadzu, Japan) was used to express the results of DSC scan (Tawfeek et al. 2020). For FT-IR, (4–5 mg, samples weight) were mixed with potassium bromide and then compressed into discs. The prepared samples placed in a sample holder and scanned from 4000 to 400 cm<sup>-1</sup> to get the FT-IR spectra (Singh et al. 2016).

### 2.3.5. In vitro release

Diffusion technique was adapted to measure the cumulative release of SUL from the selected SUL-NLC formulation using the dialysis membrane method as previously reported (Tawfeek et al. 2020; Halevas et al. 2021; Abdelfattah et al. 2022). Suspension of the selected SUL-NLC and pure SUL powder in phosphate buffer of pH 6.8 (equivalent to 2 mg/ml SUL) were gently added to a cylinder made of glass. A pre-soaked dialysis membrane (Spectra/Por<sup>®</sup>, Mw cut-off 12,000–14,000) was fitted at its lower end. This system was then immersed in a 25 ml phosphate buffer at 37 ± 0.5 °C and stirred at a constant rate of 50 rpm using Wise-Shake digital orbital shaker (SHO-2D, DAIHAN Scientific Co., Ltd, Korea). Two mL samples were taken at specified interval points (0.5, 1, 2, 3, 4, 6, 8 and 24 h), then replaced with a fresh buffer. The SUL concentration of each sample was measured spectrophotometrically at  $\lambda_{\max}$  of 293 nm using UV-VIS spectrophotometry (Shimadzu, model UV-1601 PC, Kyoto, Japan). Release experiment were done in triplicate and the obtained data were stated as the mean cumulative SUL released ± SD.

### 2.3.6. Stability study

SUL-NLC chosen formulation was subjected to physical stability investigation. Experiment was performed in the fridge (4.0 ± 1.0 °C) and at laboratory temperature (25.0 ± 2.0 °C) for 3 months with a visual inspection of the physical stability of the formulation after 1, 2 and 3 months. Visual inspection of the prepared nanosuspension includes any discoloration and or appearance of precipitate over the investigated time period. In addition, particle size, PDI, and particles charge were also measured monthly as previously mentioned (Abdellatif and Tawfeek 2016).

## 2.4. In vivo pharmacokinetics

### 2.4.1. Study design

Pharmacokinetics investigations were approved by the Ethical Approval Committee, Faculty of Pharmacy, Assiut University, Assiut, Egypt (Ref: 05-2023-009, August 2nd, 2023). Sprague-Dawley male rats, two to three months old, weighing 180–200 ± 10 g were used in the pharmacokinetic study. Rats were delivered from the Central Animal House of Assiut University, Assiut, Egypt. Rats are rested in individually ventilated cages, air

conditioned (26–28 °C, 40–60% relative humidity), located in a specifically designated place in our laboratory. Rats were divided into the used cages, 3/cage, and kept in 12 h light/dark cycle with free access to food and tap water *ad libitum*. Rats were divided into two groups, one receiving IN formulation (50 µL for each nostril by pipette and inhaled by the rats. Rat's nostril can accommodate the 50 µL of the intranasal formulation as reported from other researchers (Chen and Hu 2023). The second group received commercial SUL capsules (Dogmatil<sup>®</sup>) orally *via* the stomach tube (equivalent to 10 mg SUL/Kg (Parikhet al. 2010; Ayub 2016). Based on the drug encapsulation efficiency, the SUL dose is approximately 2 mg SUL/rat for each group. Rats received commercial SUL in the form of suspended powder in water *via* stomach tube. The rats group receiving IN formulation was acclimatized with normal saline one week before the start of the experiment. Briefly, three rats from each group were sacrificed for collection of their blood through retro-orbital plexus and brain at time points of (0.5, 1, 2, 4, 6 and 24 h).

### 2.4.2. Plasma and brain sample preparation

The collected blood samples were centrifuged at a speed of 4000 rpm for 15 min, at 4 °C to collect the plasma. SUL was then extracted from plasma using a modified extraction technique. Briefly, 50 µL of 0.25 µg/mL metoclopramide, which acts as internal standard, was added into plasma containing SUL and vortexed. Followed by addition of three mL of ethyl acetate/dichloromethane (5:1 v/v) and centrifuged at 4 °C, 4000 rpm for 10 min to perform a liquid-liquid extraction. The organic layer containing the dissolved SUL was evaporated under nitrogen stream for approximately 2 h. Subsequently, 0.2 ml of the mobile phase was added to dissolve the residue, and the sample was injected into the HPLC (Huang et al. 2002). Brain samples were first carefully rinsed with PBS and homogenized in ice-cold 0.2% acetic acid in methanol using Omni tissue master homogenizer (setting 4, 20 s) followed by addition of 50 µL of the internal standard. After centrifuging samples at 4000 rpm for 15 min, the resulting supernatant was dried under nitrogen stream at 40 °C, reconstituted with mobile phase (200 µL of 0.05 M phosphate buffer of pH 7.5), and injected into the HPLC for analysis (Mizuchi et al. 1983).

### 2.4.3. HPLC conditions

Plasma and brain Samples were analysed *via* HPLC coupled with a fluorescence detector. The fluorescence detection was set at 300 and 356 nm as excitation and emission  $\lambda_{\max}$ s, respectively. Briefly, a C-18 column (5 µm, 4.6 × 150 mm, Waters, Symmetry<sup>®</sup>) was used for separation based on a reversed phase principle. Acetonitrile: 0.01 M ammonium acetate buffer (pH 5.2) was selected as a mobile phase. To get more symmetric peaks, acetic acid at 15:85 v/v ratio and 0.3% of triethylamine was added to the prepared mobile phase to get more symmetric peaks. Finally, the flow rate was adjusted to 1.0 ml/min (Giorgi et al. 2015).

Pharmacokinetic parameters, including the peak SUL concentration ( $C_{\max}$ ) and its time ( $T_{\max}$ ), area under SUL concentration-time curve (AUC) and the mean residence time (MRT) of the investigated oral SUL capsules were determined. In addition, concentration of SUL in plasma and drug concentration-time curve (AUC) in brain after SUL-NLC IN administration were also calculated using a non-compartmental analysis by Phoenix 64 Software (WinNonlin 6.4, CERTARA). The method of residual and the slope of the terminal linear line of the curve were used to calculate the absorption rate constant ( $K_{\text{abs}}$ ) and the elimination rate constant ( $K_{\text{el}}$ ). Furthermore, the apparent half-lives of absorption and elimination ( $t_{1/2}$ ) were obtained *via* dividing 0.693 by the respective

rate constant. In addition, the trapezoidal method was adapted to calculate the  $(AUC_{0-t})$  and  $(AUMC_{0-t})$  from 0 to 24 h. The  $(AUC_{0-\infty})$  and  $(AUMC_{0-\infty})$  from time zero to infinity were calculated using Equations (2) and (3), respectively.

$$AUC_{(0-\infty)} = AUC_{(0-t)} + \frac{Ct}{K_{el}} \quad (2)$$

$$AUMC_{(0-\infty)} = AUMC_{(0-t)} + \frac{t * Ct}{K_{el}} + \frac{Ct}{K_{el}^2} \quad (3)$$

where,  $C_t$  is the final concentration of SUL detected after 24 h ( $t$ ) and  $K_{el}$  is the SUL elimination rate constant. AUC is the area under plasma concentration time profile and AUMC is the area under first moment curve. In addition, SUL mean residence time (MRT) was calculated using the following equation.

$$MRT = \frac{AUMC(0 - \infty)}{AUC(0 - \infty)} \quad (4)$$

The relative bioavailability of SUL from the SUL-NLC intranasal formulation was calculated *via* this equation:

$$\text{Relative Bioavailability (\%)} = \frac{(AUC(0 - \alpha)_{\text{Plasma}})_{\text{SUL - NLC}}}{(AUC(0 - \alpha)_{\text{PLasma}})_{\text{SUL Capsules}}} \times 100\% \quad (5)$$

## 2.5. Statistical analysis

A GraphPad Prism 10 (San Diego, CA) was used to perform the statistics in this study. Data were checked for normality and homogeneity by Shapiro–Wilk test, expressed as mean  $\pm$  SD, and parametric test was used for analysis, two-tailed unpaired  $t$ -test and one-way analysis of variance. The two-tailed unpaired  $t$ -test to determine the difference between two groups. In case of multiple groups, a one-way analysis of variance (ANOVA) test was utilized followed by Dunnett's multiple comparisons test. A GraphPad prism program was used for plots presentation. A value of  $p < 0.05$  was considered statistically significant. All experiments were performed in triplicate and data were expressed as mean  $\pm$  standard deviations.

## 3. Results

### 3.1. Preparation and characterization of SUL-NLCs

SUL-NLCs were successfully prepared using the ethanol injection method using the solid lipid compritol<sup>®</sup> 888 ATO and either oleic acid or labrafac as liquid lipids. The effect of varying the type of (PF-127 or T80) and concentrations (1% or 2%) of stabilizer on the NLC particle size, PDI, zeta potential, and EE% were presented in Table 2.

### 3.1.1. Particle size

Different liquid lipids and stabilizers with different concentrations led to different particles size values. Generally, the prepared SUL-NLCs had a particle size ranged from  $640.4 \pm 50.2$  to  $373.3 \pm 12.8$  nm as depicted in Table 2. In addition, the produced NPs have PDI values equal to and less than 0.5, which meaning a monodispersed formulation (Mudalige et al. 2019). The observed high PDI in some formulations could be attributed to the high surfactant concentration as previously reported (Pandita et al. 2009; Duong et al. 2019). It was noticed that enhancing the concentration of PF-127 from 1% (S1 and S3) to 2% (S2 and S4) non-significantly ( $p > 0.05$ ) increased the produced particle size in case of oleic acid and with labrafac. In case of T80, there is a significant ( $p < 0.05$ ) decrease in particles size with increasing the T80 concentration from 1 to 2% using oleic acid and a non-significant ( $p > 0.05$ ) decrease in particles size using labrafac.

### 3.1.2. Zeta potential

The zeta potential is a crucial factor for NPs dispersion stability which generally depends on the drug chemical nature as well as the interaction with the used lipid and surfactant. It was found that all the prepared SUL-NLCs have negative values of zeta potential as indicated in Table 2. In addition, different concentrations of stabilizer affect significantly the measured zeta potential values and produced particles with higher stability. Increasing the concentration of PF-127 from 1% to 2% significantly increased ( $p < 0.05$ ) the zeta potential from  $-14.0 \pm 0.35$  mV to  $-19.9 \pm 1.13$  mV in case of oleic acid and from  $-17.6 \pm 2.14$  mV to  $-35.4 \pm 2.25$  mV in case labrafac. Similarly, increasing the concentration of T80 from 1% to 2% resulted in a significant increase ( $p < 0.05$ ) in zeta potential from  $-24.1 \pm 2.01$  mV to  $-34.7 \pm 0.25$  mV in case of oleic acid and from  $-20.5 \pm 1.35$  mV to  $-26.1 \pm 0.35$  mV in case labrafac. It was also found that SUL-NLC formulation S4 containing labrafac, stabilized with 2% PF-127, has a significantly ( $p < 0.05$ ) higher zeta potential than formulation S2 containing oleic acid. On the contrary, formulation S6 containing oleic acid, stabilized with 2% T80, has a significantly ( $p < 0.05$ ) higher zeta potential than that observed with formulation S8 containing labrafac and 2% T80.

### 3.1.3. Encapsulation efficiencies

The prepared SUL-NLCs showed variations in the determined EE% as pointed out in the Table 2. Increasing the concentration of the emulsifiers from 1% to 2% when used in combination with oleic acid significantly ( $p < 0.05$ ) increase the EE% from  $60.7 \pm 1.8$  to  $65.8 \pm 1.4\%$  in case of PF-127 and from  $64.9 \pm 1.5$  to  $75.5 \pm 1.5\%$  in case of T80. It was also noted that the SUL EE% decreased with a higher emulsifier concentration of 2% when used in combination with labrafac as a liquid lipid where the EE% significantly ( $p < 0.05$ ) reduced from  $45.9 \pm 5.5$  to  $12.7 \pm 3.8\%$  in case of PF-127

**Table 2.** Particle size (nm)  $\pm$  SD, polydispersity, PDI  $\pm$  SD, zeta potential (mV)  $\pm$  SD, and encapsulation efficiency %  $\pm$  SD for the prepared SUL-NLCs.

Formulation	Particle size (nm) $\pm$ SD	PDI $\pm$ SD	Zeta potential (mV) $\pm$ SD	EE% $\pm$ SD
S1	526.9 $\pm$ 54.8	0.538 $\pm$ 0.076	-14.0 $\pm$ 0.35	60.7 $\pm$ 1.8
S2	584.3 $\pm$ 34.7	0.489 $\pm$ 0.033	-19.9 $\pm$ 1.13	65.8 $\pm$ 1.4
S3	590.9 $\pm$ 46.9	0.524 $\pm$ 0.058	-17.6 $\pm$ 2.14	45.9 $\pm$ 5.5
S4	640.4 $\pm$ 50.2	0.424 $\pm$ 0.068	-35.4 $\pm$ 2.25	12.7 $\pm$ 3.8
S5	461.5 $\pm$ 27.1	0.464 $\pm$ 0.012	-24.1 $\pm$ 2.01	64.9 $\pm$ 1.5
S6	373.3 $\pm$ 12.8	0.396 $\pm$ 0.013	-34.7 $\pm$ 0.25	75.5 $\pm$ 1.5
S7	377.4 $\pm$ 44.4	0.466 $\pm$ 0.190	-20.5 $\pm$ 1.35	40.6 $\pm$ 2.4
S8	366.2 $\pm$ 62.1	0.414 $\pm$ 0.143	-26.1 $\pm$ 0.35	29.6 $\pm$ 3.2

Note: Average particle size as measured by dynamic light scattering. All data are presented as the mean  $\pm$  SD ( $n = 3$ ). Abbreviations: SUL-NLC: sulphiride loaded nanostructured lipid carrier, PDI: polydispersity index; EE%: encapsulation efficiency percentage.

and from  $40.6 \pm 2.4$  to  $29.6 \pm 3.2\%$  in case of T80 as depicted in (Table 2).

### 3.1.4. TEM

Figure 1 displays TEM images of the chosen SUL-NLC formulation. These vesicles exhibit uniform, smooth, and monodisperse spherical structures with a consistent size distribution. Notably, smaller SUL-NLC particle size was observed through TEM than that measured *via* DLS. This difference can be attributed to slight particles aggregation which could be performed in aqueous NPs dispersion, whereas TEM captures homogeneous, non-aggregated particles (Elnaggar et al. 2020). This behaviour is also found with many researchers (Abdellatif, Aldosari, et al. 2022; Abdellatif et al. 2023; Tawfeek et al. 2023).

### 3.1.5. DSC analysis

DSC analysis provides a significant value in the assessment of interactions between drugs, lipids and surfactants, as well as the behaviour of mixtures involving compritol<sup>®</sup>888 ATO and oleic acid. Figure 2 shows the thermograms of SUL powder, compritol<sup>®</sup>888 ATO, physical mixture of SUL with compritol<sup>®</sup>888 ATO, blank NLC, and SUL-NLC. DSC measurement shows an endothermic peak of SUL at  $175^\circ\text{C}$  corresponding SUL melting (Tawfeek et al. 2020), proving its crystalline state (Zidan et al. 2015). Whereas, compritol<sup>®</sup>888 ATO shows sharp endothermic peaks at  $72.31^\circ\text{C}$ , representing its melting points. Physical mixture of compritol<sup>®</sup>888 ATO with SUL showed both the melting endothermic peaks. However, an obvious reduction and a little shift in the compritol<sup>®</sup>888 ATO endothermic peak was evident in the respective thermogram of both blank NLC and SUL-NLC formulations, as compared to the peak observed for pure compritol<sup>®</sup>888 ATO. SUL-NLC did not show the melting peak of SUL. In addition, it was found that the thermogram of blank NLC and SUL-NLC formulations shows a reduced and a little peak shift of compritol<sup>®</sup>888 ATO. This can be attributed to the presence of lipid particles within the colloidal size range and the interaction between solid and liquid lipids through the formulation process (Gönüllü et al. 2015).

### 3.1.6. FT-IR spectroscopy

FT-IR is a powerful tool for the superficial characterization of nano formulations. FTIR analysis was performed over the range of  $4000\text{--}400\text{ cm}^{-1}$ . Free SUL, compritol, their respective physical mixture, Blank NLC, and the selected SUL-NLC formulation were investigated for any physical or chemical interactions using FT-IR spectroscopy as presented in Figure 3. The FT-IR spectrum of SUL displays its characteristic absorption bands at  $3385\text{ cm}^{-1}$  (N-H),  $3211\text{ cm}^{-1}$  ( $-\text{NH}_2$ ),  $1643\text{ cm}^{-1}$  (C=O), and  $1322\text{ cm}^{-1}$  ( $-\text{SO}_2$ ) (Mohamad et al. 2021). The primary absorption peaks of Compritol<sup>®</sup> 888 ATO were detected at  $3300\text{ cm}^{-1}$  for O-H stretching,  $2815\text{ cm}^{-1}$  for C-H stretching, and  $1738\text{ cm}^{-1}$  for C=O stretching (Tran et al. 2014). The FTIR spectrum of the physical mixture show the distinct peaks of both SUL and compritol. The FT-IR spectra for both the blank NLC and SUL-NLC formulations exhibited nearly identical profiles. The absence of characteristic SUL peaks in the spectrum of SUL-NLC confirmed the successful incorporation of SUL into the lipid matrix (Teng et al. 2019).

### 3.1.7. In vitro SUL release

SUL released from chosen SUL-NLC formulation is presented in Figure 4. Individual dispersion of free SUL was employed as a control to confirm that the drug was readily released through the dialysis membrane and to investigate how its entrapment into NLC affects the release profile. SUL aqueous dispersion showed a cumulative SUL release of  $81.7 \pm 4.8\%$  after 3 h. On the other hand, when SUL was encapsulated within NLC, it exhibited a sustained release of SUL, with a cumulative release of  $41.8 \pm 4.6\%$  after the first 3 h. After 24 h, the percentage of drug released reached  $64.7 \pm 4.6\%$ . It was clear that at the beginning of release experiment till 2 h, there is an observed initial burst effect followed by a sustained release phase.

### 3.1.8. Stability study

Stability study of the selected SUL-NLC was performed to ensure the physical stability of the prepared SUL-NLC at two different conditions. Visual inspection of SUL-NLC stored at the refrigerator and at room temperature did not show any sedimentation or aggregations after the stated stability storage period. A slight

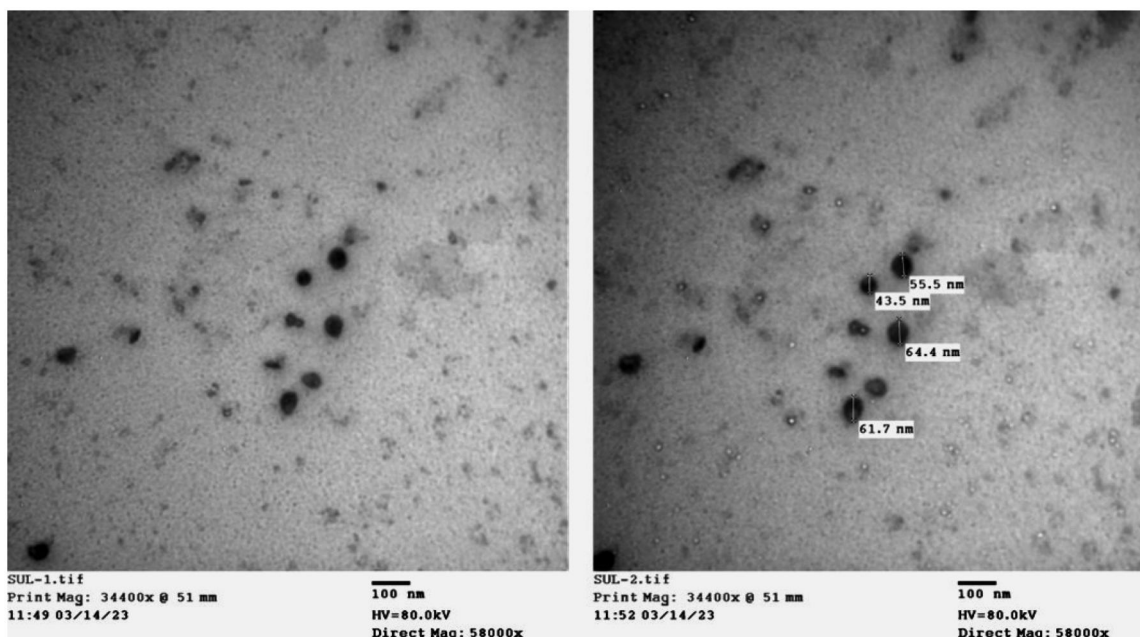


Figure 1. Representative transmission electron microscope images of the selected formulation of SUL-NLC. The scale bar represents 100 nm.

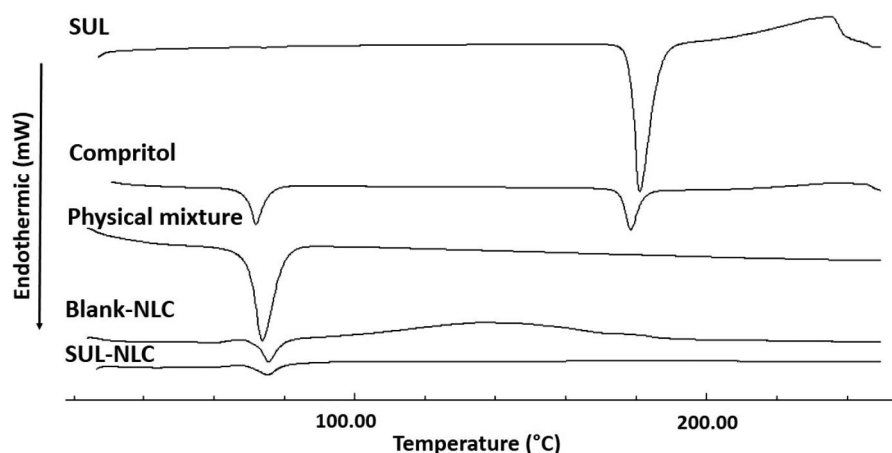


Figure 2. DSC thermogram of SUL powder, compritol<sup>®</sup>888 ATO, physical mixture of SUL with compritol<sup>®</sup>888 ATO, and blank NLC & SUL-NLC dried powders.

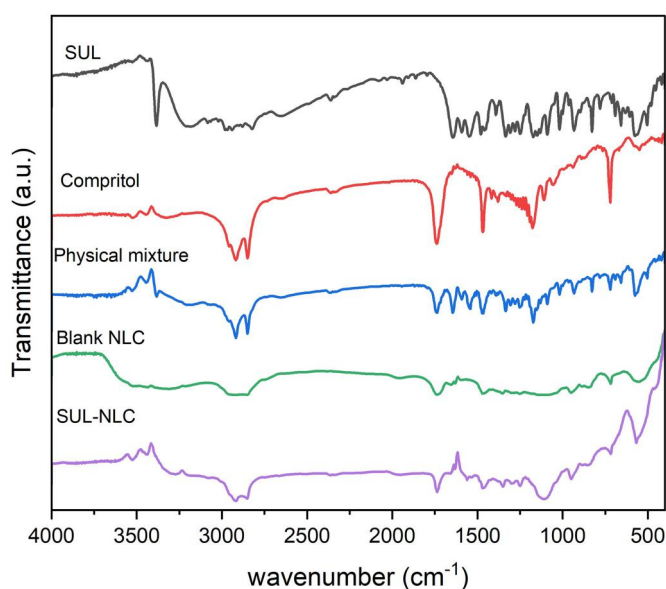


Figure 3. FT-IR spectra of SUL, compritol<sup>®</sup>888 ATO, their respective physical mixture, and blank NLC & SUL-NLC (formulation S6) dried powders.

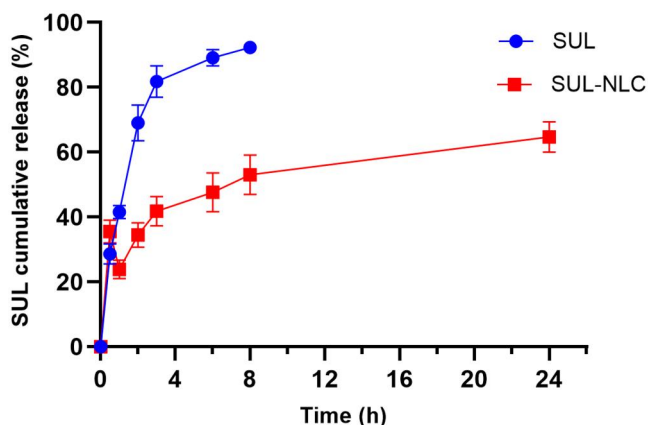


Figure 4. Cumulative percent SUL released in PBS solution of pH 7.4 at 37°C from the selected SUL-NLC in comparison to the free non-encapsulated SUL dispersion. Data are expressed as mean  $\pm$  SD ( $n = 3$ ).

non-significant ( $p > 0.05$ ) increase in particle size and PDI were observed at the investigated storage conditions, compared to the freshly prepared SUL-NLC (Table 3). The encapsulation efficiencies

of the samples after three months maintained approximately similar results ( $73.32 \pm 1.6\%$  and  $75.84 \pm 2.5\%$  in the refrigerator and at room temperature, respectively) compared to the freshly prepared formulation ( $75.5 \pm 1.5\%$ ). The stability results indicated that the SUL-NLC formulation was stable at the investigated conditions of storage during the entire period of study and the ability of NLC to hold the drug in its nano-template structure stable for three months.

### 3.2. In vivo pharmacokinetics

Within the nasal cavity, there are some important pathways which help to direct the drugs to the brain, positively impacting CNS drug pharmacokinetic/pharmacodynamic (PK/PD) profiles (Formica et al. 2022). The PK parameters of SUL in plasma after IN administration of SUL-NLC formulation and oral administration of commercial SUL product Dogmatil<sup>®</sup> capsules are presented in Table 4. Their respective plasma-SUL concentration versus time curves is depicted in Figure 5A and B. The  $C_{max}$ ,  $AUC_{0-24}$  and bioavailability of IN administered SUL-NLC were significantly higher ( $p < 0.01$ ) compared to orally administered Dogmatil<sup>®</sup> (Table 4 and Figure 5A). IN administration increased SUL  $C_{max}$  in the plasma by nearly 7.5-fold compared to oral drug administration. In addition, IN delivery demonstrated a 5-fold slower clearance from the blood, with an increased MRT to 37 h compared to oral SUL. In addition, the percentage relative bioavailability increased by 4.47-fold compared to the oral administration of commercial SUL capsules.

Effective brain delivery of SUL was achieved after IN administration of SUL-NLC, as evidenced by comparable AUC of SUL in both brain tissues and plasma which also reveals accumulation in the brain tissue. It was found that IN formulation showed a non-significantly ( $p > 0.01$ ) higher  $AUC_{0-24}$  in the brain ( $35178.38 \pm 353.7 \text{ ng.hr/ml}$ ) compared to that obtained in the plasma ( $33998.38 \pm 490 \text{ ng.hr/ml}$ ) as depicted in Figure 5B.

## 4. Discussion

The blood brain barrier as a unique barrier unable many drugs to reach the brain within considerable quantities to treat different neurological disorders (Moradi and Dashti 2022; Rauf et al. 2022). It was also found that most medications used for CNS disorders showed a minimum effect for most of their users due to the lower concentration reaching the effective site of action as well as poor absorption rates. This is why searching for effective therapeutic strategies are necessary to address these issues. NPs have

**Table 3.** Characterization of the prepared SUL-NLCs stored at refrigerator ( $4.0 \pm 0.5^\circ\text{C}$ ) and room temperature ( $25 \pm 2.0^\circ\text{C}$ ).

	Size (nm)		PDI		Zeta potential (mV)	
	286.6 $\pm$ 0.7		0.394 $\pm$ 0.012		-31.3 $\pm$ 0.889	
0 month	286.6 $\pm$ 0.7		0.394 $\pm$ 0.012		-31.3 $\pm$ 0.889	
1st month	287.8 $\pm$ 6.9*	287.1 $\pm$ 5.9**	0.41 $\pm$ 0.04*	0.38 $\pm$ 0.01**	-29.8 $\pm$ 0.05*	-29.2 $\pm$ 1.2**
2nd month	288.9 $\pm$ 3.5*	288.4 $\pm$ 4.3**	0.35 $\pm$ 0.01*	0.42 $\pm$ 0.1**	-33.3 $\pm$ 4.1*	-28.5 $\pm$ 1.3**
3rd month	292.0 $\pm$ 10.3*	289.0 $\pm$ 7.3**	0.41 $\pm$ 0.1*	0.43 $\pm$ 0.01**	-30.9 $\pm$ 1.0*	-28.3 $\pm$ 2.3**

\*Refrigerator ( $4.0 \pm 0.5^\circ\text{C}$ ).\*\*Room temperature ( $25 \pm 2.0^\circ\text{C}$ ).**Table 4.** Pharmacokinetic parameters of SUL in plasma after in administration of SUL-NLC and oral administration of commercial SUL product Dogmatil<sup>®</sup> capsules.

Pharmacokinetic parameters	SUL-NLC IN	Commercial SUL tablets	p-Value
$C_{\max 1}$ (ng/mL)	3953.1 $\pm$ 498.8	522.5 $\pm$ 27.4	** < 0.01
$T_{\max 1}$ (h)	1.0	0.5	
$C_{\max 2}$ (ng/mL)	-	490.0 $\pm$ 24.5	-
$T_{\max 2}$ (h)	-	2.0	-
$C_{\max 3}$ (ng/mL)	-	593.4 $\pm$ 33.8	-
$T_{\max 3}$ (h)	-	24.0	-
$K_{\text{abs},1}$ ( $\text{h}^{-1}$ )	1.386 $\pm$ 0.05	2.78 $\pm$ 0.23	* < 0.05
$t_{1/2 \text{ abs},1}$ (h)	0.5 $\pm$ 0.07	0.25 $\pm$ 0.09	* < 0.05
$K_{\text{abs},2}$ ( $\text{h}^{-1}$ )	-	0.693 $\pm$ 0.16	-
$t_{1/2 \text{ abs},2}$ (h)	-	1.0 $\pm$ 0.06	-
$K_{\text{abs},3}$ ( $\text{h}^{-1}$ )	-	0.057 $\pm$ 0.01	-
$t_{1/2 \text{ abs},3}$ (h)	-	12.0 $\pm$ 0.81	-
$\text{AUC}_{0-24}$ (ng.h/mL)	33998.38 $\pm$ 1150	9925 $\pm$ 365	** < 0.01
$\text{AUC}_{0-\infty}$ (ng.h/mL)	69320.79 $\pm$ 734.5	15491.55 $\pm$ 575	** < 0.01
$\text{AUMC}_{0-24}$ (ng.h <sup>2</sup> /mL)	298878.1 $\pm$ 1980	148969.1 $\pm$ 1537	** < 0.01
$\text{AUMC}_{0-\infty}$ (ng.h <sup>2</sup> /mL)	2575073 $\pm$ 3230	334752 $\pm$ 2210	** < 0.01
MRT (h)	37.15 $\pm$ 1.99	21.60 $\pm$ 2.49	** < 0.01
Clearance	0.481 $\pm$ 0.09	2.152 $\pm$ 0.05	** < 0.01
$K_{\text{el}}$ ( $\text{h}^{-1}$ )	0.02473 $\pm$ 0.004	0.1066 $\pm$ 0.016	** < 0.01
$t_{1/2 \text{ el}}$ (h)	28.03 $\pm$ 1.85	6.49 $\pm$ 0.43	** < 0.01
Relative bioavailability (%)	447.48 $\pm$ 29.5	-	

Note: Plasma concentrations results are expressed as mean  $\pm$  SD ( $n = 5$ ). The second phase of drug absorption was used to calculate  $K_{\text{el}}$ ,  $t_{1/2 \text{ el}}$ , which begins after  $T_{\max 2}$  of 2 h for SUL commercial product. \*  $p \leq 0.05$  and \*\*  $p \leq 0.001$ .

been investigated as alternative tool for the targeted delivery of medications to CNS (Eleraky et al. 2020; Cunha et al. 2021). Furthermore, they have proven effect to cross the blood brain barrier, hence superior effect on neurodegenerative diseases (Mulvihill et al. 2020; Rahman et al. 2022). In an attempt to alleviate SUL problems associated with its low oral bioavailability as well as to direct the drug to the CNS for better action and decrease the high administered dose, an IN-delivery system based on NLC was formulated. Nasal drug delivery is an established alternative to other administration routes which allows the direct delivery of drugs to the brain (Cunha et al. 2021). NLCs as an advanced delivery system than the previously fabricated SLNs is utilized herein. It was reported that nanovehicles can improve drug properties, which are considered crucial for nose-to-brain delivery and, hence, a better performance (Feng et al. 2018). NLC can be used to deliver different active pharmaceutical compounds. They demonstrated many advantages such as higher encapsulation, longer stability, and improved therapeutic efficacy compared to other NPs such as inorganic and polymeric NPs (Din et al. 2017). In addition to, NLC incorporates biocompatible lipids and surfactants within a reasonable concentration which eventually making them superior in biopharmaceutical performance (Ana et al. 2019). Interestingly, NLC can cross the blood brain barrier, their lipid content and size enable its penetration deeply into the brain tissues without further modification and ligand attachment (Tapeinos et al. 2017).

In this study, Compritol<sup>®</sup>888 ATO was chosen as a solid lipid because it showed a proven pharmaceutical application in preparation of NLCs. Compritol<sup>®</sup>888 ATO is a mixture of esters of

behenic acid and glycerol with a wide safety profile and is used successfully for IN formulations based on NLCs (Parikh et al. 2010; Agbo et al. 2021; Zafar et al. 2022). Earlier studies illustrated how altering the liquid lipids can affect the physicochemical characteristics of the resulting lipid formulations (Wu et al. 2011).

Non-ionic stabilizers facilitate steric stabilization of the NLCs by forming a protective coating layer. This reduces the possibility of particles' electrostatic repulsion, decreases the interfacial tension within nanoparticles, preventing their aggregation, and ultimately yields smaller and more stable nanoparticles (Fathi et al. 2018; da Rocha et al. 2020). Particle size of the produced NLCs could be influenced by the presence of both oleic acid and Compritol<sup>®</sup>888 ATO. Oleic acid when mixed with Compritol<sup>®</sup>888 ATO can decrease the dispersion viscosity and eventually the nanodispersion surface tension. Thus, leads to the formation of uniform, smaller size, and smooth surface NLC particles (Jenning et al. 2000; Hu et al. 2005; Khan et al. 2018). Also, utilizing a more viscous liquid lipid oleic acid (Viscosity; 40 mPa.s at  $20^\circ\text{C}$ ) in comparison to labrafac (Viscosity; 25–33 mPa.s at  $20^\circ\text{C}$ ) resulted in smaller particle size in case of using Pluronic as an emulsifier (Salimi et al. 2019). However, smaller particle size was observed with labrafac when T80 was used as an emulsifier. During the evaporation process, oil nanodroplets stability could be controlled *via* surfactant at the interface boundary between aqueous and organic phases. Therefore, there is a critical concentration of surfactant to reach the optimum particle size and PDI. When the concentration of emulsifiers increases, there is an initial decrease in both particle size and PDI. However, once the emulsifier concentration reaches a critical range, both particle size and PDI begin to increase (Duong et al. 2019).

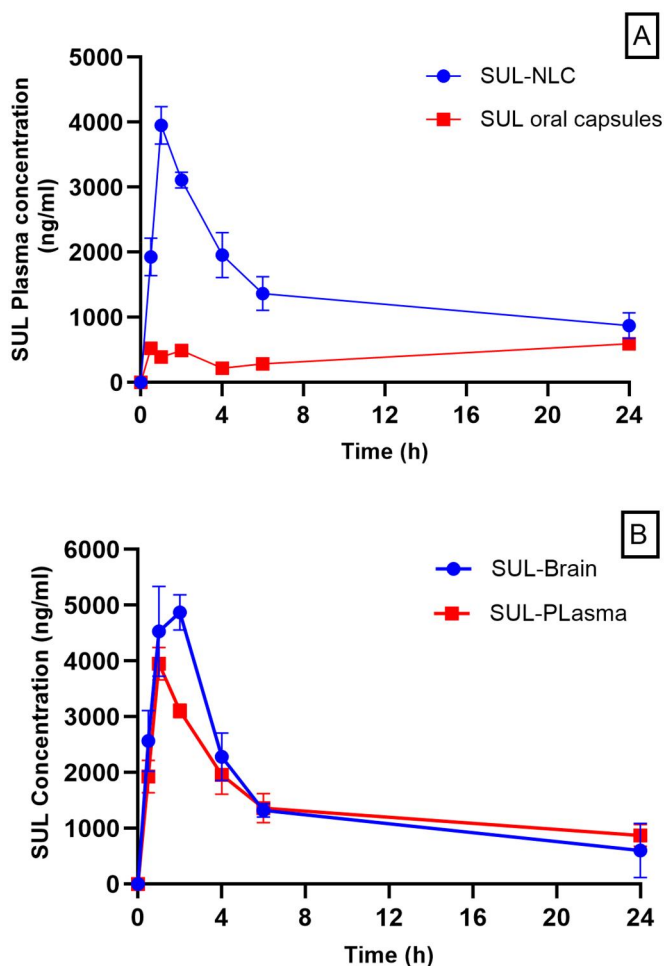


**Figure 5.** (A) Plasma-SUL concentration versus time profiles after intranasal administration of SUL-NLC and oral administration of commercial SUL capsule in Sprague Dawley rats.; and (B) Plasma and brain SUL concentration versus time profiles of SUL-NLC formulation after intranasal administration to rats ( $n = 3$ ).

The observed increases in the particles size of SUL-NLC in the case of oleic acid and labrafac when the concentration of PF-127 increased from 1% to 2% could be possibly attributed to the higher viscosity of the outer phase, which eventually reduce the diffusion rates of lipid molecules and lead to formation of bigger particles (Pandita et al. 2009; Jain et al. 2010; 2014). While, increasing the concentration of T80 from 1% to 2% showed a decrease in SUL-NLC particle size in case of oleic acid and labrafac. Lowering the interfacial tension between the lipid and aqueous phases, as the concentration of T80 increases, could be responsible for such result as reported by other researchers (Gref et al. 1995; Wu et al. 2011; Cirri et al. 2018). Generally, compritol®888 ATO produced large particles compared with other solid lipids like precirol. This behaviour is due to the composition of lipid, higher melting point, high viscosity, and a long-chain hydrocarbon (Jenning and Gohla 2000). However, as previously reported, the obtained size from formulations S6 and S8 is still suitable for brain targeting via the IN route (Aboud et al. 2016).

Formulations S4 and S6, S8 could be considered as stable formulations with zeta potential higher than 25 mV and PDI less than 0.5 as previously reported (Maqsood et al. 2022). It has been delineated from the literature that the ideal lipid based colloidal formulation should has a zeta potential in the range of  $\pm 25$  mV (Agrawal et al. 2010; Khaleeq et al. 2020). In addition, these colloidal formulations should also have a PDI value less than 0.5 to

be considered stable (Mudalige et al. 2019). The investigated two stabilizers are mainly non-ionic surfactants and generally exert their stabilizing action through steric effect they perform when located at the particle/water interface, which prevents particles agglomeration (Friedrich et al. 2015; Khosa et al. 2018). Negative zeta potential of the obtained nanosystem holds immense significance in the realm of colloid science and surface chemistry of nanoparticles. It plays a vital role in stabilizing colloidal systems, preventing particle flocculation, controlling rheological properties, enhancing drug delivery systems, and influencing surface chemistry (Abdellatif, Rasheed, et al. 2020; Abdellatif et al. 2021).

The water solubility of drugs has a crucial role during the preparation process of NLCs via the solvent injection method, NLCs containing SUL, being practically water insoluble drug, show reasonable EE% (Joshi et al. 2012; Devkar et al. 2014). Incorporation of liquid lipids into solid lipids disrupted the crystalline order significantly, creating sufficient space for SUL to be encapsulated, depending on the solubility of the drug into the lipid phase (Hu et al. 2005). Liquid lipid type significantly affects the encapsulation efficiency of NLCs, where EE% increase in case of oleic acid compared to labrafac. The higher viscosity of oleic acid compared to labrafac could be responsible for this observation which preventing the escape of the drug to the aqueous phase (Eleraky et al. 2020). This also agrees with previous studies which indicated that using oleic acid in the formulation of NLCs resulted in higher drug loading efficiency (Chinsriwongkul et al. 2012). Also, the emulsifier's type and concentration significantly affect the EE% of the NLCs. Increasing the concentration of the emulsifiers from 1% to 2% when combined with oleic acid significantly increase ( $p < 0.05$ ) the EE% in case of PF-127 and T80. Similar result was also found with levosulipride NLC prepared using oleic acid and T80 as emulsifier (Maqsood et al. 2022). The enhanced EE % may be attributed to the surfactant's dual role in improving drug solubilization inside the lipid matrix of NLCs and stabilizing role for the prepared particles. Hence, a higher surfactant concentration facilitates increased drug entrapment within the prepared NLCs (Pezeshki et al. 2014; Eleraky et al. 2020). Whereas, the observed contrary result with labrafac in case of 2% of PF-127 and T80 could be possibly attributed to the aforementioned lower viscosity of labrafac compared to oleic acid. It has been also reported that higher surfactant concentration reduced the interfacial tension between the drug and lipid which led to an increase in the EE% (Azhar Shekoufeh Bahari and Hamishehkar 2016). From the above-mentioned results, it could be concluded that formulation S6 is considered an optimum formulation in terms of lower particle size, PDI, higher zeta potential, and maximum SUL encapsulation. This formulation was used for further *in vitro* and *in vivo* studies.

TEM images represent the particle size after the removal of the hydrated layer around the particles, leading to smaller measurements compared to DLS (Abdellatif, Aldosari, et al. 2022). DLS provides the hydrodynamic diameter of hydrated vesicles in suspension, typically larger than the size of dry vesicles visualized through TEM (Mekkawy et al. 2022). It has been reported that NLC containing T80 induced crystallization that promoted self-assembly properties and reduced particles aggregation enable single particles to be easily visualized (Ariyaprakai et al. 2013; Uvanesh et al. 2016).

Compatibility of SUL with the used excipients revealed also their suitability for NLC formulation as well as gives idea about the incorporation of the drug into the lipid phase of NLC. It was clear from the DSC study that the thermogram of SUL-NLC did not show the SUL peak, thus indicates the incorporation of SUL

into the lipid phase, either as a molecular dispersion within the NLC matrix or in an amorphous state (Eleraky et al. 2020). The disappearance of the SUL peak also demonstrated the drug lipid solubilization and stability of the NLC formulation. Interaction between solid and liquid lipid could produce a less organized crystal or amorphous lipid matrix, which facilitates drug incorporation into the lipid core (Tran et al. 2014). Also, from the FT-IR results it was clearer that the absence of characteristic SUL peaks in the SUL-NLC spectrum proving the successful incorporation of SUL into the lipid phase of NLC (Teng et al. 2019; Eleraky et al. 2020; Abdellatif, Aldosari, et al. 2022).

Nasal drug delivery is designed to release the drugs in a sustained release manner (Mistry et al. 2009; Kumar et al. 2016; Rassu et al. 2016). Such behaviour of release obtained *via* nanovesicles slows down the absorption rate and can achieve stable and prolonged brain exposure. Furthermore, sustained release could enhance the nose-to-brain absorption because drug absorption *via* the circulation is reduced and relatively more absorbable drugs would be delivered directly to the brain following the migration of the nanovehicles along the nose-to-brain pathway (Feng et al. 2018). The rapid release of SUL from the aqueous suspension depended entirely on the rate at which the drug is dissolved (Mekkawy et al. 2022). SUL released from the NLC exhibited an initial burst release followed by prolonged release pattern over 24 h (Fathi et al. 2018; Khan et al. 2020; Eleraky et al. 2020). The initial burst release can be attributed to the rapid release of drug trapped near the surface of the nanoparticles, where the drug is incorporated within the liquid lipid matrix (Fathi et al. 2018). The sustained release pattern that follows is due to the lipophilic nature of SUL, which is profoundly embedded in the core matrix of the NLC. The drug's biphasic release pattern in the SUL-NLC formulation is explained by the drug's partitioning among the lipid phase and aqueous phase through the preparation process. It has been reported that during the cooling phase of the preparation of NLC process the liquid lipid deposited readily in the outer shell of NLC leaving a small fraction to be included in the inner core of the solid lipid (Hu et al. 2006). SUL-NLC utilized Compritol as a solid lipid solidifies first leading to the formation of solid lipid enriched core, where the liquid lipid accumulates in the outer layer (Hu et al. 2006). During exposure to the release medium, a small fraction of the drug present in the liquid phase is released quickly, leading to a burst effect (Shah et al. 2016). The tested SUL-NLC formulation is physically stable at the investigated two storage conditions without appreciable aggregation after three months of storage. Inclusion of T80 to the SUL-NLC stabilize the dispersion for a long time as previously mentioned through steric effect (Thatipamula et al. 2011). Similar results were also found with Singh SK et al. who demonstrated an enhanced physical stability for asenapine (5HT<sub>2A</sub> and D<sub>2</sub> receptor antagonist) loaded NLC for IN delivery to the brain when stored at room temperature (Singh et al. 2016).

Generally, non-compartmental analysis was employed to examine the PK data of SUL, since oral SUL as well as IN delivery fit this model (Younis et al. 2020). The oral SUL formulation exhibited non-linear pharmacokinetics with multiple peaks in plasma concentration due to the presence of various absorption sites in the GIT with different absorption rates, influenced by weak base nature of SUL and ionization in acidic GIT conditions which causes its lower absorption (Davies et al. 2010; Giorgi et al. 2013; Helmy 2013; Tawfeek et al. 2020; Younis et al. 2020). In contrast, IN delivery of SUL-NLC did not show such behaviour and demonstrated a more uniform PK profile, avoiding fluctuations in blood concentration with oral administration.

IN formulation showed a non-significantly ( $p > 0.01$ ) higher AUC<sub>0-24</sub> in the brain ( $35178.38 \pm 353.7$  ng.hr/ml) compared to that obtained in the plasma ( $33998.38 \pm 490$  ng.hr/ml). The sustained SUL release from the NLC is responsible for this prolonged release in brain and blood. Previous results reported higher brain concentration of asenapine, 5HT<sub>2A</sub> receptor antagonist, compared to the blood after IN administration of asenapine-NLC (Singh et al. 2016). The enhanced permeation could be attributed to the nanocarrier's constituents, including liquid lipid, T80, and the nanosized particles (Kreuter 2001; Wilson et al. 2008). Moreover, the improved brain targeting is advantageous promising route of administration, where IN delivery of SUL offered several advantages, such as avoiding P-gp efflux in the GIT, circumventing absorption windows in the upper GIT, reaching effective concentration in the brain despite being a P-gp substrate in nasal epithelium, and bypassing the blood-brain barrier to target specific receptors in the central nervous system, making it a favourable option over oral delivery (Kohri et al. 1996; Baluom et al. 2001; Graff and Pollack 2003; Hanson and Frey 2008). Interestingly, even though the drug could be a substrate for a P-gp efflux in the nasal epithelium but the presence of T80 in the chosen formulation could alleviate this issue. It has been reported that SUL self-micro emulsifying drug delivery system containing T80 can induce membrane perturbation and P-gp inhibition leading to enhance the SUL permeation (Zhang et al. 2003; Shono et al. 2004). It cannot be neglected that this study has some limitations. As it has proven in our study that IN delivery of SUL could be a non-invasive alternative for the delivery of SUL to the brain with a significant higher SUL brain concentration and bioavailability. However, pharmacodynamic studies are required to prove this statement. Histopathology study for brain tissues and immune-histochemical analysis could also be investigated. In addition, future study will take into consideration the effect of other types of lipids offering high solubility of SUL to enhance the amounts of drug loading into the NLC.

## 5. Conclusion

Nanostructured lipid carriers, due to their lipidic nature and nano sizes could be particularly efficient in delivering therapeutic agents to the brain *via* the nasal route. SUL-NLC was successfully formulated with reasonable drug encapsulation and size suitable for efficient IN delivery. Furthermore, the sustained release performance offered from the prepared SUL-NLC could enhance the nose-to-brain absorption. The prepared NLC was also stable at the investigated stability conditions emerging the suitability of this formulation. Employing a lipid carrier for the efficient encapsulation of this hydrophobic drug results in an increased in relative bioavailability by 4.47-fold compared to the oral administration of commercial SUL capsules. Consequently, the delivery of SUL through the IN route, bypassing P-gp efflux in the GIT and absorption windows located in the upper part of the GIT, coupled with the utilization of NLCs for facilitating delivery to the brain, emerges as a promising approach for enhancing the low bioavailability of SUL and managing CNS disorders.

The targeting potential could be enhanced by surface modification through utilizing charged lipids like stearylamine. In addition, NLC could be incorporated into a responsive gelling system to different triggers like ions and temperature to facilitates the application and residence time by overcoming the forces of mucociliary clearance. To conclude, NLCs is considered simple, safe, industrially scalable and efficient alternative for brain

targeting, providing a highly significance in the field of neuroscience and nanoformulation for efficient delivery of drugs to CNS.

### CRedit authorship contribution statement

**Hesham M. Tawfeek:** Supervision, Conceptualization, Methodology, Writing-original draft, Software, Validation, Project administration, Writing-review and editing. **Aml I. Mekawy:** Conceptualization, Methodology, Writing-original draft, Software, Validation, Writing-review & editing. **Ahmed A. H. Abdellatif:** Conceptualization, Methodology, Visualization, Writing- review& editing. **Basmah N. Aldosari:** Methodology, Funding acquisition, Software, Validation, Visualization, Data curation, Review and editing. **Waleed A Mohammed-Saeid:** Methodology, Funding acquisition, Software, Data curation, Review and editing. **Marwa G. Elnaggar:** Conceptualization, Methodology, Data curation, Software, Formal analysis, Writing-original draft, Writing-review & editing.

### Disclosure statement

No potential conflict of interest was reported by the authors.

### Funding

The author(s) reported there is no funding associated with the work featured in this article.

### ORCID

Hesham M. Tawfeek  <http://orcid.org/0000-0001-9789-9953>

### References

- Abdelfattah A, Aboutaleb AE, Abdel-Aal ABM, Abdellatif AAH, Tawfeek HM, Abdel-Rahman SI. 2022. Design and optimization of PEGylated silver nanoparticles for efficient delivery of doxorubicin to cancer cells. *J Drug Delivery Sci Technol.* 71:103347. doi: [10.1016/j.jddst.2022.103347](https://doi.org/10.1016/j.jddst.2022.103347).
- Abdellatif AA, Tawfeek HM. 2016. Transfersomal nanoparticles for enhanced transdermal delivery of clindamycin. *AAPS PharmSciTech.* 17(5):1067–1074. doi: [10.1208/s12249-015-0441-7](https://doi.org/10.1208/s12249-015-0441-7).
- Abdellatif AAH, Abdelfattah A, Younis MA, Aldalaan SM, Tawfeek HM. 2023. Chitosan-capped silver nanoparticles with potent and selective intrinsic activity against the breast cancer cells. *Nanotechnol Rev.* 12(1): 20220546. doi: [10.1515/ntrev-2022-0546](https://doi.org/10.1515/ntrev-2022-0546).
- Abdellatif AAH, Aldosari BN, Al-Subaiyel A, Alhaddad A, Samman WA, Eleraky NE, Elnaggar MG, Barakat H, Tawfeek HM. 2022. Transethosomal gel for the topical delivery of celecoxib: formulation and estimation of skin cancer progression. *Pharmaceutics.* 15(1):22. doi: [10.3390/pharmaceutics15010022](https://doi.org/10.3390/pharmaceutics15010022).
- Abdellatif AAH, Alhathloul SS, Aljohani ASM, Maswadeh H, Abdallah EM, Hamid Musa K, El Hamd MA. 2022. Green synthesis of silver nanoparticles incorporated aromatherapies utilized for their antioxidant and antimicrobial activities against some clinical bacterial isolates. *Bioinorg Chem Appl.* 2022(1):2432758. doi: [10.1155/2022/2432758](https://doi.org/10.1155/2022/2432758).
- Abdellatif AAH, Alturki HNH, Tawfeek HM. 2021. Different cellulosic polymers for synthesizing silver nanoparticles with antioxidant and antibacterial activities. *Sci Rep.* 11(1):84. doi: [10.1038/s41598-020-79834-6](https://doi.org/10.1038/s41598-020-79834-6).
- Abdellatif AAH, Ibrahim MA, Amin MA, Maswadeh H, Alwehaibi MN, Al-Harbi SN, Alharbi ZA, Mohammed HA, Mehany ABM, Saleem I. 2020. Cetuximab conjugated with octreotide and entrapped calcium alginate-beads for targeting somatostatin receptors. *Sci Rep.* 10(1):4736. doi: [10.1038/s41598-020-61605-y](https://doi.org/10.1038/s41598-020-61605-y).
- Abdellatif AAH, Rasheed Z, Alhowail AH, Alqasoumi A, Alsharidah M, Khan RA, Aljohani ASM, Aldubayan MA, Faisal W. 2020. Silver citrate nanoparticles inhibit PMA-induced TNFalpha expression via deactivation of NF-kappaB activity in human cancer cell-lines, MCF-7. *Int J Nanomedicine.* 15:8479–8493. doi: [10.2147/IJN.S274098](https://doi.org/10.2147/IJN.S274098).
- Abdellatif AAH, Tolba NS, Alsharidah M, Al Rugaie O, Bouazzaoui A, Saleem I, Maswadeh H, Ali AT. 2022. PEG-4000 formed polymeric nanoparticles loaded with cetuximab downregulate p21 & stathmin-1 gene expression in cancer cell lines. *Life Sci.* 295: 120403. doi: [10.1016/j.lfs.2022.120403](https://doi.org/10.1016/j.lfs.2022.120403).
- Abdulla NA, Balata GF, El-Ghamry HA, Gomaa E. 2021. Intranasal delivery of Clozapine using nanoemulsion-based in-situ gels: an approach for bioavailability enhancement. *Saudi Pharm J.* 29(12):1466–1485. doi: [10.1016/j.jsps.2021.11.006](https://doi.org/10.1016/j.jsps.2021.11.006).
- Aboud HM, El Komy MH, Ali AA, El Menshawe SF, Abd Elbary A. 2016. Development, optimization, and evaluation of carvedilol-loaded solid lipid nanoparticles for intranasal drug delivery. *AAPS PharmSciTech.* 17(6):1353–1365. doi: [10.1208/s12249-015-0440-8](https://doi.org/10.1208/s12249-015-0440-8).
- Achar A, Myers R, Ghosh C. 2021. Drug delivery challenges in brain disorders across the blood-brain barrier: novel methods and future considerations for improved therapy. *Biomedicines.* 9(12):1834. eng. doi: [10.3390/biomedicines9121834](https://doi.org/10.3390/biomedicines9121834).
- Agbo CP, Ugwuanyi TC, Ugwuoke WI, McConville C, Attama AA, Ofokansi KC. 2021. Intranasal artesunate-loaded nanostructured lipid carriers: a convenient alternative to parenteral formulations for the treatment of severe and cerebral malaria. *J Control Release.* 334:224–236. doi: [10.1016/j.jconrel.2021.04.020](https://doi.org/10.1016/j.jconrel.2021.04.020).
- Agrawal Y, Petkar KC, Sawant KK. 2010. Development, evaluation and clinical studies of Acitretin loaded nanostructured lipid carriers for topical treatment of psoriasis. *Int J Pharm.* 401(1-2):93–102. doi: [10.1016/j.ijpharm.2010.09.007](https://doi.org/10.1016/j.ijpharm.2010.09.007).
- Aldosari BN, Abd El-Aal M, Abo Zeid EF, Faris TM, Aboeela A, Abdellatif AAH, Tawfeek HM. 2023. Synthesis and characterization of magnetic Ag-Fe(3)O(4)@polymer hybrid nanocomposite systems with promising antibacterial application. *Drug Dev Ind Pharm.* 49(12):723–733. doi: [10.1080/03639045.2023.2277812](https://doi.org/10.1080/03639045.2023.2277812).
- Ana R, Mendes M, Sousa J, Pais A, Falcão A, Fortuna A, Vitorino C. 2019. Rethinking carbamazepine oral delivery using polymer-lipid hybrid nanoparticles. *Int J Pharm.* 554:352–365. doi: [10.1016/j.ijpharm.2018.11.028](https://doi.org/10.1016/j.ijpharm.2018.11.028).
- Ariyaprakai S, Limpachoti T, Pradipasena P. 2013. Interfacial and emulsifying properties of sucrose ester in coconut milk emulsions in comparison with Tween. *Food Hydrocolloids.* 30(1): 358–367. doi: [10.1016/j.foodhyd.2012.06.003](https://doi.org/10.1016/j.foodhyd.2012.06.003).
- Ayub AMA. 2016. Intranasal microemulgel as surrogate carrier to enhance low oral bioavailability of sulpiride. *Innovare Acad Sci.* 10:188–197.
- Azhar Shekoufeh Bahari L, Hamishehkar H. 2016. The impact of variables on particle size of solid lipid nanoparticles and nanostructured lipid carriers; a comparative literature review. *Adv Pharm Bull.* 6(2):143–151. doi: [10.15171/apb.2016.021](https://doi.org/10.15171/apb.2016.021).
- Baluom M, Friedman M, Rubinstein A. 2001. Improved intestinal absorption of sulpiride in rats with synchronized oral delivery systems. *J Control Release.* 70(1-2):139–147. doi: [10.1016/s0168-3659\(00\)00337-0](https://doi.org/10.1016/s0168-3659(00)00337-0).
- Bourganis V, Kammona O, Alexopoulos A, Kiparissides C. 2018. Recent advances in carrier mediated nose-to-brain delivery of

- pharmaceutics. *Eur J Pharm Biopharm.* 128:337–362. doi: [10.1016/j.ejpb.2018.05.009](https://doi.org/10.1016/j.ejpb.2018.05.009).
- Chen K, Hu X. 2023. Intranasal creatine administration increases brain creatine level and improves Barnes maze performance in rats. *Brain Res Bull.* 201:110703. doi: [10.1016/j.brainresbull.2023.110703](https://doi.org/10.1016/j.brainresbull.2023.110703).
- Chen Y, Yuan L, Zhou L, Zhang ZH, Cao W, Wu Q. 2012. Effect of cell-penetrating peptide-coated nanostructured lipid carriers on the oral absorption of tripterine. *Int J Nanomedicine.* 7:4581–4591. eng. doi: [10.2147/IJN.S34991](https://doi.org/10.2147/IJN.S34991).
- Chinsriwongkul A, Chareanputtakhun P, Ngawhirunpat T, Rojanarata T, Sila-On W, Ruktanonchai U, Opanasopit P. 2012. Nanostructured lipid carriers (NLC) for parenteral delivery of an anticancer drug. *Aaps Pharmscitech.* 13(1):150–158. doi: [10.1208/s12249-011-9733-8](https://doi.org/10.1208/s12249-011-9733-8).
- Chitneni M, Peh KK, Darwis D, Abdulkarim M, Abdullah GZ, Qureshi MJ. 2011. Intestinal permeability studies of sulpiride incorporated into self-microemulsifying drug delivery system (SMEDDS). *Pak J Pharm Sci.* 24(2):113–121.
- Cirri M, Maestrini L, Maestrelli F, Mennini N, Mura P, Ghelardini C, Di Cesare Mannelli L. 2018. Design, characterization and in vivo evaluation of nanostructured lipid carriers (NLC) as a new drug delivery system for hydrochlorothiazide oral administration in pediatric therapy. *Drug Deliv.* 25(1):1910–1921. doi: [10.1080/10717544.2018.1529209](https://doi.org/10.1080/10717544.2018.1529209).
- Cunha S, Forbes B, Sousa Lobo JM, Silva AC. 2021. Improving drug delivery for Alzheimer's disease through nose-to-brain delivery using nanoemulsions, nanostructured lipid carriers (NLC) and in situ hydrogels. *Int J Nanomedicine.* 16:4373–4390. doi: [10.2147/IJN.S305851](https://doi.org/10.2147/IJN.S305851).
- da Rocha MCO, da Silva PB, Radicchi MA, Andrade BYG, de Oliveira JV, Venus T, Merker C, Estrela-Lopis I, Longo JPF, Bão SN. 2020. Docetaxel-loaded solid lipid nanoparticles prevent tumor growth and lung metastasis of 4T1 murine mammary carcinoma cells. *J Nanobiotechnology.* 18(1):43. doi: [10.1186/s12951-020-00604-7](https://doi.org/10.1186/s12951-020-00604-7).
- Davies NM, Takemoto JK, Brocks DR, Yáñez JA. 2010. Multiple peaking phenomena in pharmacokinetic disposition. *Clin Pharmacokinet.* 49(6):351–377. doi: [10.2165/11319320-000000000-00000](https://doi.org/10.2165/11319320-000000000-00000).
- Deshkar SS, Jadhav MS, Shirolkar SV. 2021. Development of carbamazepine nanostructured lipid carrier loaded thermosensitive gel for intranasal delivery. *Adv Pharm Bull.* 11(1):150–162. doi: [10.34172/apb.2021.016](https://doi.org/10.34172/apb.2021.016).
- Devkar TB, Tekade AR, Khandelwal KR. 2014. Surface engineered nanostructured lipid carriers for efficient nose to brain delivery of ondansetron HCl using Delonix regia gum as a natural mucoadhesive polymer. *Colloids Surf B Biointerfaces.* 122:143–150. doi: [10.1016/j.colsurfb.2014.06.037](https://doi.org/10.1016/j.colsurfb.2014.06.037).
- Din FU, Aman W, Ullah I, Qureshi OS, Mustapha O, Shafique S, Zeb A. 2017. Effective use of nanocarriers as drug delivery systems for the treatment of selected tumors. *Int J Nanomedicine.* 12:7291–7309. doi: [10.2147/IJN.S146315](https://doi.org/10.2147/IJN.S146315).
- Duong V-A, Nguyen T-T-L, Maeng H-J, Chi S-C. 2019. Preparation of ondansetron hydrochloride-loaded nanostructured lipid carriers using solvent injection method for enhancement of pharmacokinetic properties. *Pharm Res.* 36(10):138. doi: [10.1007/s11095-019-2672-x](https://doi.org/10.1007/s11095-019-2672-x).
- Eleraky N, Omar M, Mahmoud H, Abou-Taleb H. 2020. Nanostructured lipid carriers to mediate brain delivery of temazepam: design and in vivo study. *Pharmaceutics.* 12(5):451. doi: [10.3390/pharmaceutics12050451](https://doi.org/10.3390/pharmaceutics12050451).
- Elmaggar MG, Jiang K, Eldesouky HE, Pei Y, Park J, Yuk SA, Meng F, Dieterly AM, Mohammad HT, Hegazy YA, et al. 2020. Antibacterial nanotruffles for treatment of intracellular bacterial infection. *Biomaterials.* 262:120344. eng. doi: [10.1016/j.biomaterials.2020.120344](https://doi.org/10.1016/j.biomaterials.2020.120344).
- Fathi HA, Allam A, Elsbahy M, Fetih G, El-Badry M. 2018. Nanostructured lipid carriers for improved oral delivery and prolonged antihyperlipidemic effect of simvastatin. *Colloids Surf B Biointerfaces.* 162:236–245. doi: [10.1016/j.colsurfb.2017.11.064](https://doi.org/10.1016/j.colsurfb.2017.11.064).
- Feng Y, He H, Li F, Lu Y, Qi J, Wu W. 2018. An update on the role of nanovehicles in nose-to-brain drug delivery. *Drug Discov Today.* 23(5):1079–1088. doi: [10.1016/j.drudis.2018.01.005](https://doi.org/10.1016/j.drudis.2018.01.005).
- Formica ML, Real DA, Picchio ML, Catlin E, Donnelly RF, Paredes AJ. 2022. On a highway to the brain: a review on nose-to-brain drug delivery using nanoparticles. *Appl Mater Today.* 29:101631. doi: [10.1016/j.apmt.2022.101631](https://doi.org/10.1016/j.apmt.2022.101631).
- Friedrich RB, Kann B, Coradini K, Offerhaus HL, Beck RCR, Windbergs M. 2015. Skin penetration behavior of lipid-core nanocapsules for simultaneous delivery of resveratrol and curcumin. *Eur J Pharm Sci.* 78:204–213. doi: [10.1016/j.ejps.2015.07.018](https://doi.org/10.1016/j.ejps.2015.07.018).
- Giorgi M, Ozdemir M, Camillo F, Panzani D. 2013. Pharmacokinetics of sulpiride after intravenous, intramuscular, and oral single-dose administration in nurse mares. *J Equine Vet Sci.* 33(7):533–538. doi: [10.1016/j.jevs.2012.08.005](https://doi.org/10.1016/j.jevs.2012.08.005).
- Giorgi M, Vullo C, De Vito V, Catone G, Faillace V, Laus F. 2015. Pharmacokinetic evaluations of sulpiride after intravenous, intramuscular, and oral single-dose administration in jennies (*Equus asinus*). *J Equine Vet Sci.* 35(1):13–18. doi: [10.1016/j.jevs.2014.10.003](https://doi.org/10.1016/j.jevs.2014.10.003).
- Gönüllü Ü, Üner M, Yener G, Karaman EF, Aydoğmuş Z. 2015. Formulation and characterization of solid lipid nanoparticles, nanostructured lipid carriers and nanoemulsion of lornoxicam for transdermal delivery. *Acta Pharm.* 65(1):1–13. doi: [10.1515/acph-2015-0009](https://doi.org/10.1515/acph-2015-0009).
- Graff CL, Pollack GM. 2003. P-Glycoprotein attenuates brain uptake of substrates after nasal instillation. *Pharm Res.* 20(8):1225–1230. doi: [10.1023/a:1025053115583](https://doi.org/10.1023/a:1025053115583).
- Gref R, Domb A, Quellec P, Blunk T, Müller R, Verbavatz J-M, Langer R. 1995. The controlled intravenous delivery of drugs using PEG-coated sterically stabilized nanospheres. *Adv Drug Deliv Rev.* 16(2-3):215–233. doi: [10.1016/0169-409X\(95\)00026-4](https://doi.org/10.1016/0169-409X(95)00026-4).
- Halevas E, Kokotidou C, Zaimai E, Moschona A, Lialiaris E, Mittraki A, Lialiaris T, Pantazaki A. 2021. Evaluation of the hemocompatibility and anticancer potential of poly ( $\epsilon$ -Caprolactone) and poly (3-Hydroxybutyrate) microcarriers with encapsulated chrysin. *Pharmaceutics.* 13(1):109. doi: [10.3390/pharmaceutics13010109](https://doi.org/10.3390/pharmaceutics13010109).
- Hanson LR, Frey WH. 2008. Intranasal delivery bypasses the blood-brain barrier to target therapeutic agents to the central nervous system and treat neurodegenerative disease. *BMC Neurosci.* 9(Suppl 3):S5. doi: [10.1186/1471-2202-9-S3-S5](https://doi.org/10.1186/1471-2202-9-S3-S5).
- Helmy SA. 2013. Therapeutic drug monitoring and pharmacokinetic compartmental analysis of sulpiride double-peak absorption profile after oral administration to human volunteers. *Biopharm Drug Dispos.* 34(5):288–301. doi: [10.1002/bdd.1843](https://doi.org/10.1002/bdd.1843).
- Hu F-Q, Jiang S-P, Du Y-Z, Yuan H, Ye Y-Q, Zeng S. 2005. Preparation and characterization of stearic acid nanostructured lipid carriers by solvent diffusion method in an aqueous system. *Colloids Surf B Biointerfaces.* 45(3-4):167–173. doi: [10.1016/j.colsurfb.2005.08.005](https://doi.org/10.1016/j.colsurfb.2005.08.005).

- Hu F-Q, Jiang S-P, Du Y-Z, Yuan H, Ye Y-Q, Zeng S. 2006. Preparation and characteristics of monostearin nanostructured lipid carriers. *Int J Pharm.* 314(1):83–89. doi: [10.1016/j.ijpharm.2006.01.040](https://doi.org/10.1016/j.ijpharm.2006.01.040).
- Huang M-C, Ho H-O, Yeh G-C, Ke W-T, Lin L-C, Hsu T, Sheu M-T. 2002. Application of HPLC method using normal phase column in a comparative pharmacokinetic study of two sulpiride tablet formulations. *J Food Drug Anal.* 10(1):5.
- Ibrahim WM, AlOmran AH, B Yassin AE. 2014. Novel sulpiride-loaded solid lipid nanoparticles with enhanced intestinal permeability. *Int J Nanomedicine.* 9:129–144. doi: [10.2147/IJN.S54413](https://doi.org/10.2147/IJN.S54413).
- Jain A, Mishra SK, Vuddanda PR, Singh SK, Singh R, Singh S. 2014. Targeting of diacerein loaded lipid nanoparticles to intra-articular cartilage using chondroitin sulfate as homing carrier for treatment of osteoarthritis in rats. *Nanomedicine.* 10(5):e1031–e1040. doi: [10.1016/j.nano.2014.01.008](https://doi.org/10.1016/j.nano.2014.01.008).
- Jain AK, Jain A, Garg NK, Agarwal A, Jain A, Jain SA, Tyagi RK, Jain RK, Agrawal H, Agrawal GP. 2014. Adapalene loaded solid lipid nanoparticles gel: an effective approach for acne treatment. *Colloids Surf B Biointerfaces.* 121:222–229. doi: [10.1016/j.colsurfb.2014.05.041](https://doi.org/10.1016/j.colsurfb.2014.05.041).
- Jain S, Jain S, Khare P, Gulbake A, Bansal D, Jain SK. 2010. Design and development of solid lipid nanoparticles for topical delivery of an anti-fungal agent. *Drug Deliv.* 17(6):443–451. doi: [10.3109/10717544.2010.483252](https://doi.org/10.3109/10717544.2010.483252).
- Jenning V, Gohla S. 2000. Comparison of wax and glyceride solid lipid nanoparticles (SLN). *Int J Pharm.* 196(2):219–222. doi: [10.1016/s0378-5173\(99\)00426-3](https://doi.org/10.1016/s0378-5173(99)00426-3).
- Jenning V, Thünemann AF, Gohla SH. 2000. Characterisation of a novel solid lipid nanoparticle carrier system based on binary mixtures of liquid and solid lipids. *Int J Pharm.* 199(2):167–177. doi: [10.1016/s0378-5173\(00\)00378-1](https://doi.org/10.1016/s0378-5173(00)00378-1).
- Jicsinszky L, Martina K, Cravotto G. 2021. Cyclodextrins in the antiviral therapy. *J Drug Deliv Sci Technol.* 64:102589. doi: [10.1016/j.jddst.2021.102589](https://doi.org/10.1016/j.jddst.2021.102589).
- Joshi AS, Patel HS, Belgamwar VS, Agrawal A, Tekade AR. 2012. Solid lipid nanoparticles of ondansetron HCl for intranasal delivery: development, optimization and evaluation. *J Mater Sci Mater Med.* 23(9):2163–2175. doi: [10.1007/s10856-012-4702-7](https://doi.org/10.1007/s10856-012-4702-7).
- Khaleeq N, Din F, Khan AS, Rabia S, Dar J, Khan GM. 2020. Development of levosulpiride-loaded solid lipid nanoparticles and their in vitro and in vivo comparison with commercial product. *J Microencapsul.* 37(2):160–169. doi: [10.1080/02652048.2020.1713242](https://doi.org/10.1080/02652048.2020.1713242).
- Khan A, Imam SS, Aqil M, Ahad A, Sultana Y, Ali A, Khan K. 2016. Brain targeting of temozolomide via the intranasal route using lipid-based nanoparticles: brain pharmacokinetic and scintigraphic analyses. *Mol Pharm.* 13(11):3773–3782. doi: [10.1021/acs.molpharmaceut.6b00586](https://doi.org/10.1021/acs.molpharmaceut.6b00586).
- Khan AA, Abdulbaqi IM, Abou Assi R, Murugaiyah V, Darwis Y. 2018. Lyophilized hybrid nanostructured lipid carriers to enhance the cellular uptake of verapamil: statistical optimization and in vitro evaluation. *Nanoscale Res Lett.* 13(1):323. doi: [10.1186/s11671-018-2744-6](https://doi.org/10.1186/s11671-018-2744-6).
- Khan N, Shah FA, Rana I, Ansari MM, Din FU, Rizvi SZH, Aman W, Lee G-Y, Lee E-S, Kim J-K, et al. 2020. Nanostructured lipid carriers-mediated brain delivery of carbamazepine for improved in vivo anticonvulsant and anxiolytic activity. *Int J Pharm.* 577:119033. doi: [10.1016/j.ijpharm.2020.119033](https://doi.org/10.1016/j.ijpharm.2020.119033).
- Khosa A, Reddi S, Saha RN. 2018. Nanostructured lipid carriers for site-specific drug delivery. *Biomed Pharmacother.* 103:598–613. doi: [10.1016/j.biopha.2018.04.055](https://doi.org/10.1016/j.biopha.2018.04.055).
- Kim DS, Kim DW, Kim KS, Choi JS, Seo YG, Youn YS, Oh KT, Yong CS, Kim JO, Jin SG, et al. 2016. Development of a novel l-sulpiride-loaded quaternary microcapsule: effect of TPGS as an absorption enhancer on physicochemical characterization and oral bioavailability. *Colloids Surf B Biointerfaces.* 147:250–257. doi: [10.1016/j.colsurfb.2016.08.010](https://doi.org/10.1016/j.colsurfb.2016.08.010).
- Kim J, Ahn SI, Kim Y. 2019. Nanotherapeutics engineered to cross the blood-brain barrier for advanced drug delivery to the central nervous system. *J Ind Eng Chem.* 73:8–18. doi: [10.1016/j.jiec.2019.01.021](https://doi.org/10.1016/j.jiec.2019.01.021).
- Kohri N, Naasani I, Iseki K, Miyazaki K. 1996. Improving the oral bioavailability of sulpiride by a gastric-retained form in rabbits. *J Pharm Pharmacol.* 48(4):371–374. doi: [10.1111/j.2042-7158.1996.tb05935.x](https://doi.org/10.1111/j.2042-7158.1996.tb05935.x).
- Kozlovskaya L, Abou-Kaoud M, Stepensky D. 2014. Quantitative analysis of drug delivery to the brain via nasal route. *J Control Release.* 189:133–140. doi: [10.1016/j.jconrel.2014.06.053](https://doi.org/10.1016/j.jconrel.2014.06.053).
- Kreuter J. 2001. Nanoparticulate systems for brain delivery of drugs. *Adv Drug Deliv Rev.* 47(1):65–81. doi: [10.1016/s0169-409x\(00\)00122-8](https://doi.org/10.1016/s0169-409x(00)00122-8).
- Kumar A, Pandey AN, Jain SK. 2016. Nasal-nanotechnology: revolution for efficient therapeutics delivery. *Drug Deliv.* 23(3):681–693. doi: [10.3109/10717544.2014.920431](https://doi.org/10.3109/10717544.2014.920431).
- Tawfeek H, Hassan YA, Aldawsari MF, H. Fayed M. 2020. Enhancing the low oral bioavailability of sulpiride via fast orally disintegrating tablets: formulation, optimization and in vivo characterization. *Pharmaceuticals.* 13(12):446. doi: [10.3390/ph13120446](https://doi.org/10.3390/ph13120446).
- Maqsood S, Din FU, Khan SU, Elahi E, Ali Z, Jamshaid H, Zeb A, Nadeem T, Ahmed W, Khan S, et al. 2022. Levosulpiride-loaded nanostructured lipid carriers for brain delivery with anti-psychotic and antidepressant effects. *Life Sci.* 311(Pt B):121198. doi: [10.1016/j.lfs.2022.121198](https://doi.org/10.1016/j.lfs.2022.121198).
- Mekkiawy AI, Eleraky NE, Soliman GM, Elnaggar MG, Elnaggar MG. 2022. Combinatorial therapy of letrozole- and quercetin-loaded spanlastics for enhanced cytotoxicity against MCF-7 breast cancer cells. *Pharmaceutics.* 14(8):1727. doi: [10.3390/pharmaceutics14081727](https://doi.org/10.3390/pharmaceutics14081727).
- Mistry A, Stolnik S, Illum L. 2009. Nanoparticles for direct nose-to-brain delivery of drugs. *Int J Pharm.* 379(1):146–157. doi: [10.1016/j.ijpharm.2009.06.019](https://doi.org/10.1016/j.ijpharm.2009.06.019).
- Mizuchi A, Kitagawa N, Miyachi Y. 1983. Regional distribution of sultopride and sulpiride in rat brain measured by radioimmunoassay. *Psychopharmacology (Berl).* 81(3):195–198. doi: [10.1007/BF00427261](https://doi.org/10.1007/BF00427261).
- Mohamad SA, Safwat MA, Elrehany M, Maher SA, Badawi AM, Mansour HF. 2021. A novel nasal co-loaded loratadine and sulpiride nanoemulsion with improved downregulation of TNF- $\alpha$ , TGF- $\beta$  and IL-1 in rabbit models of ovalbumin-induced allergic rhinitis. *Drug Deliv.* 28(1):229–239. doi: [10.1080/10717544.2021.1872741](https://doi.org/10.1080/10717544.2021.1872741).
- Mohyeldin SM, Samy WM, Ragab D, Abdelmonsif DA, Aly RG, Elgindy NA. 2021. Precisely fabricated sulpiride-loaded nanoliposomes with ameliorated oral bioavailability and antidepressant activity. *Int J Nanomedicine.* 16:2013–2044. doi: [10.2147/IJN.S296726](https://doi.org/10.2147/IJN.S296726).
- Moradi F, Dashti N. 2022. Targeting neuroinflammation by intranasal delivery of nanoparticles in neurological diseases: a comprehensive review. *Naunyn Schmiedebergs Arch Pharmacol.* 395(2):133–148. doi: [10.1007/s00210-021-02196-x](https://doi.org/10.1007/s00210-021-02196-x).
- Mudalige T, Qu H, Van Haute D, Ansar SM, Paredes A, Ingle T. 2019. Chapter 11 – Characterization of nanomaterials: tools and challenges. In: López Rubio A, Fabra Rovira MJ, Martínez Sanz

- M editors. *Nanomaterials for food applications*. Elsevier; p. 313–353.
- Mulvihill JJ, Cunnane EM, Ross AM, Duskey JT, Tosi G, Grabruker AM. 2020. Drug delivery across the blood–brain barrier: recent advances in the use of nanocarriers. *Nanomedicine (Lond)*. 15(2):205–214. doi: [10.2217/nnm-2019-0367](https://doi.org/10.2217/nnm-2019-0367).
- Nakazato T, Horikawa HP, Akiyama A. 1998. The dopamine D2 receptor antagonist sulpiride causes long-lasting serotonin release. *Eur J Pharmacol*. 363(1):29–34. doi: [10.1016/s0014-2999\(98\)00796-1](https://doi.org/10.1016/s0014-2999(98)00796-1).
- Nance E, Pun SH, Saigal R, Sellers DL. 2022. Drug delivery to the central nervous system. *Nat Rev Mater*. 7(4):314–331. doi: [10.1038/s41578-021-00394-w](https://doi.org/10.1038/s41578-021-00394-w).
- Noorulla KM, Yasir M, Muzaffar F, R S, Ghoneim MM, Almurshedi AS, Tura AJ, Alshehri S, Gebissa T, Mekit S, et al. 2022. Intranasal delivery of chitosan decorated nanostructured lipid carriers of Buspirone for brain targeting: formulation development, optimization and in-vivo preclinical evaluation. *J Drug Delivery Sci Technol*. 67:102939. doi: [10.1016/j.jddst.2021.102939](https://doi.org/10.1016/j.jddst.2021.102939).
- Pandita D, Ahuja A, Velpandian T, Lather V, Dutta T, Khar R. 2009. Characterization and in vitro assessment of paclitaxel loaded lipid nanoparticles formulated using modified solvent injection technique. *Die Pharm*. 64(5):301–310.
- Pardeike J, Hommoss A, Müller RH. 2009. Lipid nanoparticles (SLN, NLC) in cosmetic and pharmaceutical dermal products. *Int J Pharm*. 366(1-2):170–184. eng. doi: [10.1016/j.ijpharm.2008.10.003](https://doi.org/10.1016/j.ijpharm.2008.10.003).
- Parikh T, Bommana MM, Squillante E. 2010. Efficacy of surface charge in targeting pegylated nanoparticles of sulpiride to the brain. *Eur J Pharm Biopharm*. 74(3):442–450. doi: [10.1016/j.ejpb.2009.11.001](https://doi.org/10.1016/j.ejpb.2009.11.001).
- Patel M, Souto EB, Singh KK. 2013. Advances in brain drug targeting and delivery: limitations and challenges of solid lipid nanoparticles. *Expert Opin Drug Deliv*. 10(7):889–905. doi: [10.1517/17425247.2013.784742](https://doi.org/10.1517/17425247.2013.784742).
- Patel S, Chavhan S, Soni H, Babbar AK, Mathur R, Mishra AK, Sawant K. 2011. Brain targeting of risperidone-loaded solid lipid nanoparticles by intranasal route. *J Drug Target*. 19(6):468–474. doi: [10.3109/1061186X.2010.523787](https://doi.org/10.3109/1061186X.2010.523787).
- Pezechki A, Ghanbarzadeh B, Mohammadi M, Fathollahi I, Hamishehkar H. 2014. Encapsulation of vitamin A palmitate in nanostructured lipid carrier (NLC)-effect of surfactant concentration on the formulation properties. *Adv Pharm Bull*. 4(Suppl 2): 563–568. doi: [10.5681/apb.2014.083](https://doi.org/10.5681/apb.2014.083).
- Rahman MM, Islam MR, Akash S, Harun-Or-Rashid M, Ray TK, Rahaman MS, Islam M, Anika F, Hosain MK, Aovi FI, et al. 2022. Recent advancements of nanoparticles application in cancer and neurodegenerative disorders: at a glance. *Biomed Pharmacother*. 153:113305. doi: [10.1016/j.biopha.2022.113305](https://doi.org/10.1016/j.biopha.2022.113305).
- Rassu G, Soddu E, Cossu M, Gavini E, Giunchedi P, Dalpiaz A. 2016. Particulate formulations based on chitosan for nose-to-brain delivery of drugs. A review. *J Drug Delivery Sci Technol*. 32:77–87. doi: [10.1016/j.jddst.2015.05.002](https://doi.org/10.1016/j.jddst.2015.05.002).
- Rassu G, Soddu E, Posadino AM, Pintus G, Sarmento B, Giunchedi P, Gavini E. 2017. Nose-to-brain delivery of BACE1 siRNA loaded in solid lipid nanoparticles for Alzheimer's therapy. *Colloids Surf B Biointerfaces*. 152:296–301. doi: [10.1016/j.colsurfb.2017.01.031](https://doi.org/10.1016/j.colsurfb.2017.01.031).
- Rauf A, Badoni H, Abu-Izneid T, Olatunde A, Rahman MM, Painuli S, Semwal P, Wilairatana P, Mubarak MS. 2022. Neuroinflammatory markers: key indicators in the pathology of neurodegenerative diseases. *Molecules*. 27(10):3194. doi: [10.3390/molecules27103194](https://doi.org/10.3390/molecules27103194).
- Salimi A, Zadeh BSM, Kazemi M. 2019. Preparation and optimization of polymeric micelles as an oral drug delivery system for deferoxamine mesylate: in vitro and ex vivo studies. *Res Pharm Sci*. 14(4):293–307. doi: [10.4103/1735-5362.263554](https://doi.org/10.4103/1735-5362.263554).
- Shah NV, Seth AK, Balaraman R, Aundhia CJ, Maheshwari RA, Parmar GR. 2016. Nanostructured lipid carriers for oral bioavailability enhancement of raloxifene: design and in vivo study. *J Adv Res*. 7(3):423–434. doi: [10.1016/j.jare.2016.03.002](https://doi.org/10.1016/j.jare.2016.03.002).
- Shono Y, Nishihara H, Matsuda Y, Furukawa S, Okada N, Fujita T, Yamamoto A. 2004. Modulation of intestinal P-glycoprotein function by cremophor EL and other surfactants by an in vitro diffusion chamber method using the isolated rat intestinal membranes. *J Pharm Sci*. 93(4):877–885. doi: [10.1002/jps.20017](https://doi.org/10.1002/jps.20017).
- Singh SK, Dadhania P, Vuddanda PR, Jain A, Velaga S, Singh S. 2016. Intranasal delivery of asenapine loaded nanostructured lipid carriers: formulation, characterization, pharmacokinetic and behavioural assessment. *RSC Adv*. 6(3):2032–2045. doi: [10.1039/C5RA19793G](https://doi.org/10.1039/C5RA19793G).
- Tapeinos C, Battaglini M, Ciofani G. 2017. Advances in the design of solid lipid nanoparticles and nanostructured lipid carriers for targeting brain diseases. *J Control Release*. 264:306–332. doi: [10.1016/j.jconrel.2017.08.033](https://doi.org/10.1016/j.jconrel.2017.08.033).
- Tawfeek HM, Abdellatif AAH, Abdel-Aleem JA, Hassan YA, Fathalla D. 2020. Transfersomal gel nanocarriers for enhancement the permeation of lornoxicam. *J Drug Delivery Sci Technol*. 56: 101540. doi: [10.1016/j.jddst.2020.101540](https://doi.org/10.1016/j.jddst.2020.101540).
- Tawfeek HM, Younis MA, Aldosari BN, Almurshedi AS, Abdelfattah A, Abdel-Aleem JA. 2023. Impact of the functional coating of silver nanoparticles on their in vivo performance and biosafety. *Drug Dev Ind Pharm*. 49(5):349–356. doi: [10.1080/03639045.2023.2214207](https://doi.org/10.1080/03639045.2023.2214207).
- Teng Z, Yu M, Ding Y, Zhang H, Shen Y, Jiang M, Liu P, Opoku-Damoah Y, Webster TJ, Zhou J. 2019. Preparation and characterization of nimodipine-loaded nanostructured lipid systems for enhanced solubility and bioavailability. *Int J Nanomedicine*. 14:119–133. doi: [10.2147/IJN.S186899](https://doi.org/10.2147/IJN.S186899).
- Terstappen GC, Meyer AH, Bell RD, Zhang W. 2021. Strategies for delivering therapeutics across the blood–brain barrier. *Nat Rev Drug Discov*. 20(5):362–383. doi: [10.1038/s41573-021-00139-y](https://doi.org/10.1038/s41573-021-00139-y).
- Thatipamula R, Palem C, Gannu R, Mudragada S, Yamsani M. 2011. Formulation and in vitro characterization of domperidone loaded solid lipid nanoparticles and nanostructured lipid carriers. *Daru*. 19(1):23.
- Tran TH, Ramasamy T, Truong DH, Choi H-G, Yong CS, Kim JO. 2014. Preparation and characterization of fenofibrate-loaded nanostructured lipid carriers for oral bioavailability enhancement. *AAPS Pharmscitech*. 15(6):1509–1515. doi: [10.1208/s12249-014-0175-y](https://doi.org/10.1208/s12249-014-0175-y).
- Uvanesh K, Sagiri SS, Banerjee I, Shaikh H, Pramanik K, Anis A, Pal K. 2016. Effect of tween 20 on the properties of stearate oleogels: an in-depth analysis. *J Americ Oil Chem Soc*. 93(5):711–719. doi: [10.1007/s11746-016-2810-0](https://doi.org/10.1007/s11746-016-2810-0).
- Watanabe K, Sawano T, Terada K, Endo T, Sakata M, Sato J. 2002. Studies on intestinal absorption of sulpiride (1): carrier-mediated uptake of sulpiride in the human intestinal cell line Caco-2. *Biol Pharm Bull*. 25(7):885–890. doi: [10.1248/bpb.25.885](https://doi.org/10.1248/bpb.25.885).
- Wilson B, Samanta MK, Santhi K, Kumar KPS, Paramakrishnan N, Suresh B. 2008. Poly (n-butylcyanoacrylate) nanoparticles coated with polysorbate 80 for the targeted delivery of rivastigmine into the brain to treat Alzheimer's disease. *Brain Res*. 1200:159–168. doi: [10.1016/j.brainres.2008.01.039](https://doi.org/10.1016/j.brainres.2008.01.039).
- Wu L, Zhang J, Watanabe W. 2011. Physical and chemical stability of drug nanoparticles. *Adv Drug Deliv Rev*. 63(6):456–469. doi: [10.1016/j.addr.2011.02.001](https://doi.org/10.1016/j.addr.2011.02.001).
- Yasir M, Zafar A, Noorulla KM, Tura AJ, Sara UVS, Panjwani D, Khalid M, Haji MJ, Gobena WG, Gebissa T, et al. 2022. Nose to brain delivery of donepezil through surface modified NLCs: formulation

- development, optimization, and brain targeting study. *J Drug Delivery Sci Technol.* 75:103631. doi: [10.1016/j.jddst.2022.103631](https://doi.org/10.1016/j.jddst.2022.103631).
- Younis MA, El-Zahry MR, Tallat MA, Tawfeek HM. 2020. Sulpiride gastro-retentive floating microsponges; analytical study, in vitro optimization and in vivo characterization. *J Drug Target.* 28(4): 386–397. doi: [10.1080/1061186X.2019.1663526](https://doi.org/10.1080/1061186X.2019.1663526).
- Zafar A, Awad Alsaidan O, Alruwaili NK, Sarim Imam S, Yasir M, Saad Alharbi K, Singh L, Muqtader Ahmed M. 2022. Formulation of intranasal surface engineered nanostructured lipid carriers of rotigotine: full factorial design optimization, in vitro characterization, and pharmacokinetic evaluation. *Int J Pharm.* 627:122232. doi: [10.1016/j.ijpharm.2022.122232](https://doi.org/10.1016/j.ijpharm.2022.122232).
- Zhang H, Yao M, Morrison RA, Chong S. 2003. Commonly used surfactant, Tween 80, improves absorption of P-glycoprotein substrate, digoxin, in rats. *Arch Pharm Res.* 26(9):768–772. doi: [10.1007/BF02976689](https://doi.org/10.1007/BF02976689).
- Zidan AS, Emam SE, Shehata TM, Ghazy F-e 2015. Pediatric suppositories of sulpiride solid dispersion for treatment of Tourette syndrome: in vitro and in vivo investigations. *AAPS PharmSciTech.* 16(3):645–655. doi: [10.1208/s12249-014-0250-4](https://doi.org/10.1208/s12249-014-0250-4).